M.Tech (Power Electronics and Systems)

Mayank Ojha

2023

INVESTIGATIONS ON DIFFERENT GLOBAL PEAK TRACKING ALGORITHMS FOR EXTRACTING MAXIMUM POWER FROM PHOTOVOLTAIC SYSTEMS

DISSERTATION/THESIS

SUBMITTED IN PARTIAL FULFILLMENT OF THE REQUIREMENTS FOR THE AWARD OF THE DEGREE

OF

MASTER OF TECHNOLOGY

IN

POWER ELECTRONICS AND SYSTEMS

Submitted by:

MAYANK OJHA

2K21/PES/09

Under the supervision of

Dr. VANJARI VENKATA RAMANA

(Assistant Professor, EED, DTU)

DEPARTMENT OF ELECTRICAL ENGINEERING

DELHI TECHNOLOGICAL UNIVERSITY

(Formerly Delhi College of Engineering)

Bawana Road, Delhi-110042

2023

DEPARTMENT OF ELECTRICAL ENGINEERING

DELHI TECHNOLOGICAL UNIVERSITY

DECLARATION

I, Mayank Ojha, Roll No. 2K20/PES/09 student of M.Tech (Power Electronics and Systems), hereby declare that the project Dissertation titled **"Investigations on Different Global Peak Tracking Algorithms for extracting maximum power from Photovoltaic systems"** which is submitted by me to the Department of Electrical Engineering Department, Delhi Technological University, Delhi in partial fulfilment of the requirement for the award of the degree of Master of Technology, is original work and not previously used for the award of any Degree.

Place: Delhi
Date: 31st May, 2023

Mayank Ojha
2K21/PES/09
M.Tech (PES)

DEPARTMENT OF ELECTRICAL ENGINEERING

DELHI TECHNOLOGICAL UNIVERSITY

SUPERVISOR'S CERTIFICATE

This is to certify that the dissertation entitled **"Investigations on Different Global Peak Tracking Algorithms for extracting maximum power from Photovoltaic systems**" being submitted by Mayank Ojha (2K21/PES/09) in partial fulfillment of the requirements for the award of Master of Technology degree in "ELECTRICAL ENGINEERING" with specialization of "POWER ELECTRONICS & SYSTEMS" at the Delhi Technological University is an authentic work carried out by him under my supervision and guidance.

To the best of my knowledge, the matter embodied in the thesis has not been submitted to any other University/ Institute for the award of any degree or diploma.

Supervisor's Signature

Dr. Vanjari Venkata Ramana
Assistant Professor
Electrical Engineering Department
Delhi Technological University

Date: 31-05-2022
Place: Delhi

ACKNOWLEDGEMENT

I take this opportunity to express my deepest gratitude and appreciation to my project supervisor **Dr Vanjari Venkata Ramana**, Assistant Professor, Delhi Technological university and Head of Department **Prof. (Dr.) Pragati Kumar**, Delhi Technological university for their everlasting support.

I am thankful to him for suggesting the various aspects of the problem and project, rendering help during fabrication of work and rendering encouragement during the various phases of work.

I would like to thank my friends and all those who have helped me and encouraged me in completion of my dissertation in time.

Finally, I thank my parents for their moral support and confidence which they showed in me to pursue M. Tech at the advanced stage of my academic career.

Mayank ojha

2K21/PES/09

M.Tech (Power Electronics & Systems)

ABSTRACT

Photovoltaic (PV) systems have been emerged as promising source of energy. The optimal operation of a photovoltaic (PV) system is essential for maximizing power extraction from the PV source. To achieve this, a maximum power point tracking (MPPT) algorithm is employed in conjunction with a DC-DC converter. However, two key challenges arise when using a converter: (1) locating the maximum power point (MPP) and (2) ensuring reliable performance of the PV model under varying weather conditions. Therefore, the design of the converter plays a crucial role. This research focuses on two objectives related to non-isolated boost converters. Firstly, it involves determining the values of specific parameters such as input capacitor, output capacitor, and inductor. Secondly, it employs state-space modeling with averaging techniques to derive governing equations.

Secondly, Identifying the different global peak tracking (GPT) algorithms for tracking peak power of PV array along with their comparison. Various MPPT methods have certain merits and demerits. Under non-uniform shading conditions, which involves change in environmental conditions like irradiance, many tracking techniques abort to track the global peak power (GPP) under partial shading conditions (PSC). Therefore, investigations are done under non uniform shading conditions considering conventional MPPT techniques compared with the modified MPPT algorithms to highlight the performance of different techniques. Simulation results comparing the effectiveness of the conventional Particle Swarm Optimization (PSO), Adaptive PSO and Hybrid PO-PSO, Modified Hybrid PO & PSO have been done and it indicates that algorithms discussed here achieve global peak. A simulation model for 250W and 500 W maximum power with a practical boost converter along with MPPT controller is used for investigation using MATLAB Simulink.

Table of Contents

LIST OF FIGURES

LIST OF TABLES

NOMENCLATURE

PV	Photo Voltaic
MPPT	Maximum Power Point Tracking
DC	Direct current
CCM	Continuous Conduction Mode
PSO	Particle Swarm Optimization
P & O	Perturb and observe
V_{oc} (OCV)	Open Circuit Voltage
I_{sc} (SCC)	Short Circuit Current
M_{pp}	Maximum Power Point
N_s	No of Cells in series in a Module
N_{ss}	No of series connected Modules in a string
ΔI	Change in current
ΔP	Change in Power
ΔP_m	Change in maximum power
d_{min}	Minimum Value of Duty
d_{max}	Maximum Value of Duty
f_s	Switching Frequency
G	Irradiance
I_{pv}	Input PV current
Io_{max}	Minimum Value of Load current
Io_{min}	Maximum Value of Load current
I_{ref}	High Frequency Transformer
R_p	Parallel Resistance
Q	Electron charge
R_s	Series Resistance
R_{Load}	Equivalent Load Resistance
V_{mp}	Voltage at Maximum power point
V_{ref}	Reference Voltage
V_o	Output Voltage

CHAPTER 1

INTRODUCTION

1.1 Background

Photovoltaic panels are extensively employed in decentralized power generation. However, the performance of these systems can be significantly affected by partial shading conditions, which can result in decreased energy yield and efficiency. This is mainly due to the mismatch between the maximum power point and the operating point which varies with shading conditions. The PV system characteristics are greatly dependent on the environmental conditions[30]. The PV arrays are exposed to shaded conditions due to the surroundings such as buildings, tree shade etc. Under such circumstances, the P-V characteristics manifest multiple powers [1] due to different environmental factors such as shading etc. Different cells in the modules work according to different shading patterns. Hierarchy of the PV array shown in Fig. 1 presents multiple PV cells forms a module and a collection of modules form an Array. The efficiency of a PV device is dependent on the spectral distribution of solar radiation upon these cells.

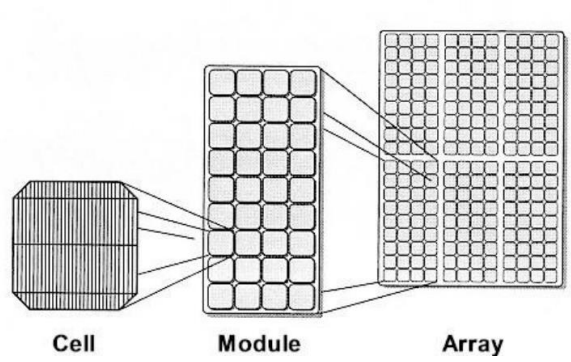

Fig. 1.1. *Hierarchy in PV Array*

Different converter configurations are utilized to link these energy sources with the power grid. However, these converters are typically designed for operation with a steady voltage source. Consequently, when connected to a variable voltage source such as a photovoltaic panel, their performance may deviate from the intended behavior. This project revolves the study about the investigations done using different algorithms for maximizing power via

MPPT coming from Manufacturer specifications typically do not include certain details about photovoltaic (PV) panels.

Firstly, using the dynamic modelling of a practical boost converter model is designed for PV panels, with the effects of varying duty cycle are examined via frequency response by deriving the transfer functions via SSA. Additionally, the impacts of temperature and partial shading on the PV panel's output are investigated. Subsequently, a boost converter is specifically designed for the PV panel, positioned between the panel and the load, to enable control through a maximum power point tracking (MPPT) controller. The PV system characteristics are greatly dependent on the environmental conditions. The PV arrays are exposed to shaded conditions due to the surroundings such as buildings, tree shade etc. Under such circumstances, the *P-V* characteristics manifest multiple powers [1]. To solve the issue of partial shading, several maximum power point tracking (MPPT) techniques were proposed to track the maximum power from each PV module and optimize the energy yield of the system [1]-[8].

Some classic MPPT algorithms, such as the Perturb and Observe (P&O) method and Incremental Conductance, cannot distinguish between local maximum points and global maximum points. Therefore, it is not possible to track the GMPP using conventional methods under conditions of partial shading. The hybrid technique proposed in [17] has the advantage of having a reduced tracking time, however its main disadvantage is the fact that it needs a voltage reference controller. Nevertheless, in order to address the challenges posed by traditional algorithms, numerous investigations have been conducted to apply MPPT techniques using computational intelligence algorithms. These include approaches utilizing fuzzy logic [9], evolutionary algorithms [10], particle swarm optimization [11], and the shuffled frog jumping algorithm [12]. All these techniques, it concludes global maximum power point tracking (GMPPT) is a promising approach that can identify the global MPP of the entire PV system, even in the presence of partial shading [7]. A comparative analysis of different GMPPT techniques for partial shading conditions is presented. The performance of the techniques is evaluated under different shading conditions. The comparison is made among

the particle swarm optimization (PSO) techniques with the conventional PSO [11], modified versions of PSO like hybrid PO-PSO[13] and adaptive PSO[8]. The literature contains the conventional PSO and some improved versions that are used to track the GMPP in PV systems subjected to partial shading [13]-[15]. In [16], it has been seen that the disadvantage of PSO is the high tracking time and the large search space.

The simulation results show that the GMPPT techniques outperform the conventional MPPT techniques in terms of energy harvest. Specifically, the PSO based GMPPT techniques improve the energy harvest of the PV system as compared to conventional MPPT techniques. Therefore, the proposed study suggests that GMPPT techniques, particularly the non-linear optimization-based algorithm, are promising for designing efficient and cost-effective PV systems.

1.2 PV System

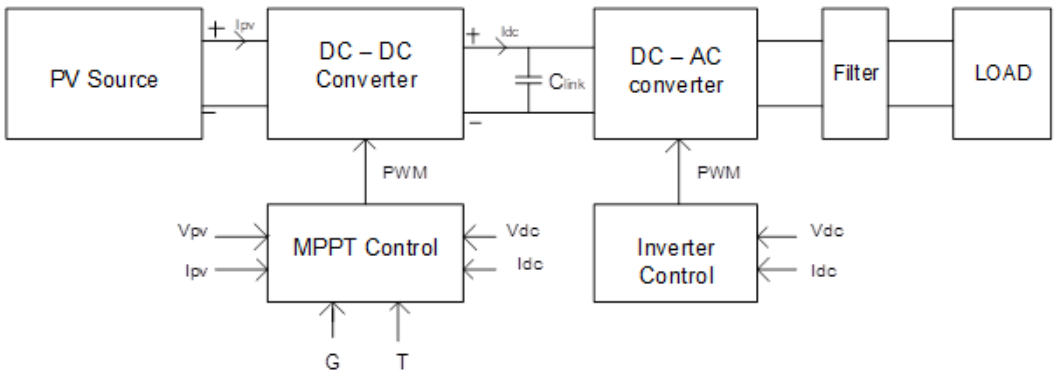

Fig. 1.2. *Generalized diagram of PV system*

The solar photovoltaic (PV) system, also known as solar PV, has been developed to harness the sun's energy and convert it into electricity using solar panels. This technology offers numerous advantages such as environmental friendliness, safety, and the generation of clean energy without contributing to pollution. Photovoltaic systems are available in different sizes and find applications in various areas including solar water heating, ventilation, lighting.

Three main categories of solar PV systems exist: grid-connected, hybrid, and off-grid. These systems utilize different techniques to convert the sun's energy into solar power and supply electricity to customers.

1. ***Grid-connected PV systems***: Also known as utility-interactive PV systems, these modules use a grid-tied inverter. The PV solar energy is converted into AC power through the inverter, reducing overall electricity consumption. Grid-connected systems allow for the possibility of feeding excess energy back into the grid.
2. ***Hybrid PV systems:*** These modules are an adapted variant of grid-connected systems and incorporate a battery backup. They are designed to work in conjunction with diesel generators, allowing for the conversion of energy into AC or DC voltage. Hybrid systems provide the advantage of stored energy for use during periods of low sunlight or power outages.
3. ***Off-grid PV systems:*** These systems are suitable for individuals or locations where grid connection is not feasible due to geographical constraints or high costs. Off-grid systems function independently and

incorporate batteries to store excess energy for use when sunlight is limited.

By offering different features and capabilities, these solar PV systems cater to various energy needs and address specific requirements based on grid availability, backup power requirements, and geographical limitations[29].

The PV system is showed in Fig. 1.2. The components presented are as follows:

1. **PV source:** A Source contains PV modules which are formed from stack of cells that absorb irradiance. The group of modules stacked either in Series or parallel form an Array. On a commercial scale, modules present are either Monocrystalline or Polycrystalline.
2. **Power converter:** Depending on the specific need, the power converter can be configured as DC to AC, DC to DC, AC to DC, and so on. DC – AC is used for Grid connection, DC – DC is used for Stepping up or down voltage at the output.
3. **MPPT control:** For maximum power point tracking, algorithms are used by taking Temperature (T), irradiance (G), Voltage (V) or current (I) as inputs. In this thesis, we have taken Current and Voltage as an input which is compared with the reference current thus providing a duty cycle which is passed to the switch for controlling the output.
4. **Filters:** Filters are used in electrical systems to selectively allow or reject certain frequencies or frequency ranges in signals. They are designed to remove unwanted noise, harmonics, or interference and to ensure the integrity and quality of the desired signals**.** In Solar PV system, DC link capacitor is used to store and smooth energy in a DC power system. It acts as an energy reservoir, supplying power during transient periods and maintaining stable voltage levels in the DC link.

1.3 MPPT Concept

MPPT is a technique used in PV systems to continuously track and operate the solar panels at their maximum power point, ensuring efficient energy conversion. Solar panels have a nonlinear voltage-current characteristic, and their maximum power point (MPP) varies with

changing environmental conditions such as sunlight intensity, temperature, and shading. The MPPT algorithm dynamically adjusts the operating point of the PV system to extract the maximum available power from the panels under varying conditions.

By employing MPPT, the system operates at the voltage and current combination that maximizes the power output. This optimization allows for increased energy harvesting and improved overall system performance. MPPT algorithms utilize various methods such as perturb and observe (P&O), incremental conductance, and hill climbing to continuously monitor and adjust the operating voltage or current to track the MPP.

The MPPT algorithm typically measures the PV panel's voltage (*V*) and current (*I*), and based on these measurements, calculates the power output. It then compares the calculated power with the previous value to determine the direction to adjust the operating point for reaching the MPP. This process is repeated continuously to adapt to changing environmental conditions and maintain the PV system's operation at its peak efficiency.

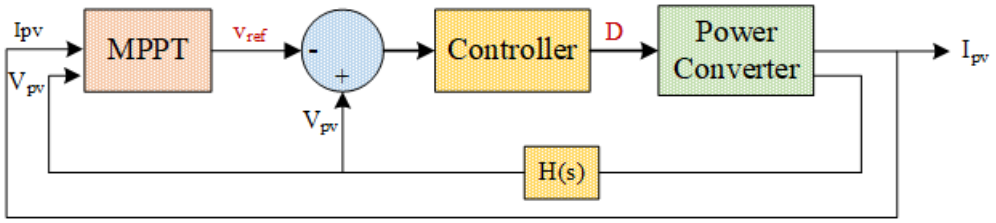

Fig. 1.3 *Schematic for MPPT controller*

The algorithm takes inputs such as PV voltage and PV current, irradiance and temperature, or a combination of these factors. It produces outputs in the form of *d*, V_{pv}, or I_{pv}.

When implementing direct duty ratio control, the duty ratio that is calculated is transmitted to the pulse width modulation (PWM) system to generate pulses responsible for controlling the converter.

To summarize, the MPPT control algorithm can take different inputs (*V*, *I*) depending on the available parameters, and it produces output in the form of duty ratio or reference voltage/current. The generated duty ratio is

used for pulse generation in direct duty ratio control, while in voltage or current reference control, a PI controller is employed to compare the reference values with the PV voltage/current, with the PWM utilizing the PI controller's output to generate pulses.

1.4 Main Objective of Research

The main objective of this work includes:

1. ***Design and Modelling of the PV System.*** The design of PV system will involve two stages as designing of converter for a specified rating, check for its stability in different conduction modes and secondly, applying MPPT controller for maximizing output of PV power.
2. ***Design and modelling of Boost converter.*** We will use a practical Boost converter for stepping up the voltage level. The converter can operate in two different modes of operation with its applicability. The study for ideal & practical boost converter will be done by deriving Small Signal Analysis model to see the changes of Voltage (V) and Current (I) with respect to Duty cycle (d)
3. ***MPPT control techniques and Algorithms.*** After designing of converter, we will learn about different MPPT techniques used in PV systems. We will shift towards the Global MPPT techniques for non-uniform shading pattern or partial shading and explore the algorithms and its usage.
4. ***Investigation via different GMPPT algorithms with MATLAB-Simulink Implementation.*** With the help of design parameters that are calculated and MPPT control algorithms, output waveforms will be obtained and further we will draw a comparison table between our studied methods to reach on a conclusion based on our research. The study is done on MATLAB-Simulink version 2020a

1.5 Outline of dissertation

The dissertation consists of the following chapters:

Chapter 1: This chapter will give an outline for the PV system and its components. Also, the concept of MPPT along with the step procedure of

major objective of our research

Chapter 2: This chapter includes the literature survey of the project "Investigations on Different Global Peak Tracking Algorithms for extracting maximum power from Photovoltaic systems". This chapter gives outline about Algorithms which have been used in MPPT for partial shading.

Chapter 3: This chapter will provide the first work which involve designing of boost converter along with its stability analysis by varying duty cycle. It includes the modelling via Small Signal Analysis and deriving transfer function for ideal & practical converter and finding out its frequency response using bode plots and step response.

Chapter 4: This Chapter will give insights about the MPPT controller and different algorithms used in it. Three algorithms which have been discussed as Conventional Particle Swarm Optimization (PSO), Adaptive Particle Swarm Optimization (APSO) and Lastly Hybrid Perturb and Observe combined with PSO.

Chapter 5: In this chapter, the simulation results will be displayed done via MATLAB Simulink will be presented here. The output waveforms for Voltage, Power, Duty cycle will be explained here. Also, the comparison analysis of all three discussed algorithms will be done form their output waveform results.

Chapter 6: In this chapter, conclusion drawn from our performed study will be presented here. The future scope of the work will the challenges will be explained there.

CHAPTER 2

LITERATURE REVIEW

2.1 Introduction

The growing need for sustainable energy sources has driven notable progress in solar photovoltaic (PV) systems. Optimizing power generation from PV systems is essential for effective energy conversion. This review summarizes the existing studies on global maximum power point tracking (MPPT) methods for solar PV systems and explores the practical application of boost converters in these systems

2.2 Overview Boost Converters in Solar PV Systems:

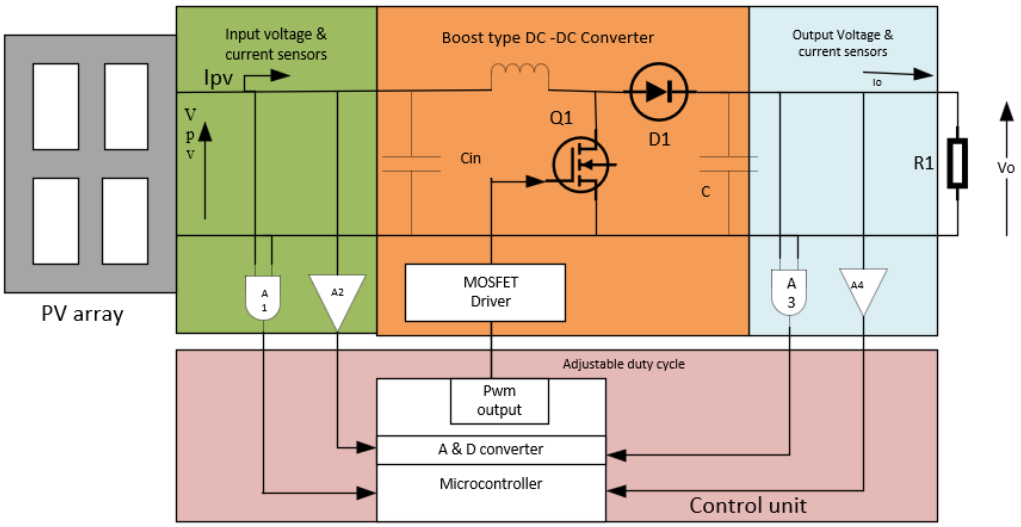

Fig 2.1. *Schematic diagram for PV system with converter and MPPT controller*

Fig 2.1 shows the Schematic diagram for PV system with converter and MPPT controller. Boost converters are extensively employed in solar PV systems to effectively convert and regulate the voltage output from solar panels. These converters play a vital role in increasing the low-voltage DC output from the panels to a higher voltage level suitable for various applications like grid connection or battery charging. Here is an overview of boost converters utilized in solar PV systems:

1. **Operational Principle:** Boost converters consist of key components such as an

inductor, diode, switch (typically a MOSFET), and capacitor. During the switch's ON state, energy is stored in the inductor by creating a magnetic field. When the switch turns off, the stored energy is released, causing the inductor voltage to reverse and deliver current to the load through the diode. By controlling the switch's duty cycle, the output voltage is regulated.

2. **Voltage Step-Up**: Boost converters offer the capability to increase the voltage, enabling the output voltage to exceed the input voltage. This is achieved by storing energy in the inductor during the switch's ON period (*Ton*) and transferring it to the load during the switch's OFF period (*Toff*).
3. **Maximum Power Point Tracking (MPPT):** Boost converters are frequently combined with MPPT algorithms to achieve the highest power extraction from solar panels. These algorithms continually monitor the solar panel's maximum power point by adapting the duty cycle of the boost converter to align the panel's impedance with the load impedance. This guarantees optimal performance of the solar panel, enabling it to generate maximum power output.
4. **Efficiency and Non-Idealities**: Boost converters in solar PV systems address non-idealities such as switching losses, conduction losses, and parasitic elements to achieve high conversion efficiency. Techniques like soft switching, synchronous rectification, and careful component selection are employed to minimize losses and enhance overall system efficiency.
5. **Protection and Safety:** Boost converters used in solar PV systems incorporate protective measures to safeguard against overvoltage, overcurrent, and short-circuit conditions. These protective features help prevent damage to system components and ensure safe operation.

Buck and buck-boost converters have their applications in other power electronics systems, boost converters are the preferred choice in PV systems due to their ability to step up the voltage, compatibility with MPPT algorithms, better voltage regulation, higher energy efficiency, and alignment with the specific requirements of PV system design. Comparison table is drawn in table I for disadvantages.

TABLE I. COMPARISION OF VARIOUS DC-DC CONVERTERS [28]

CONVERTER	OUTPUT	DISADVANTAGE
Buck	$V_o = DV_I$	Discontinuous input current, high input voltage ripple, high stress across device.
Boost	$V_o = \frac{V_i}{(1-D)}$	Discontinuous output current, high ripple in input voltage, high stress across device.
Buck-Boost	$-V_o = \frac{DV_i}{(1-D)}$	High ripple in input voltage, high stress across device, negative output voltage

*V_o = Output Voltage, V_i = Input Voltage, D = Duty Ratio

2.3 Overview of Solar PV with mismatching conditions

2.3.1 Uniform shading conditions

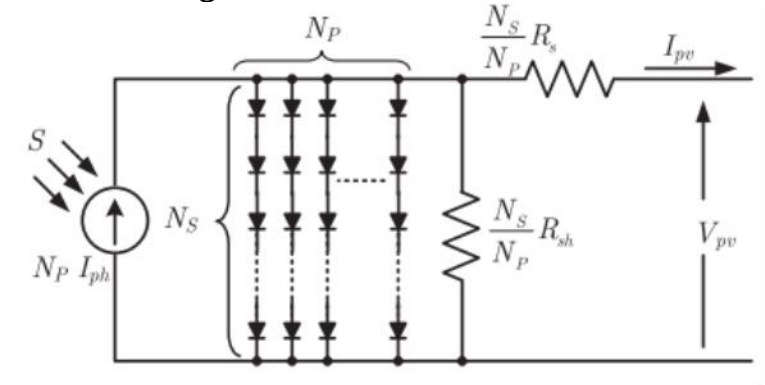

Fig 2.2. *Generalized model of PV cell*

In a uniform condition, when all the modules in a photovoltaic (PV) system are interconnected in series, they demonstrate identical electrical characteristics. The configuration depicted in Figure 2.2 illustrates a system composed of N_{ss} modules connected in series and N_{pp} strings connected in parallel. Therefore, the equation representing the system can be adjusted accordingly. Equation of current *I* can be written as (2.1). Solving the value of I in (2.2), we can obtain the I -V characteristics for the

PV module. The 3 points in the curve such as Maximum power point (*mpp*), Open circuit Voltage (V_{oc}) and Short circuit Current (I_{sc}) are defined. At OCV, $V = Voc$ and $I = 0$. Whereas at SCC, $V = 0$ and $I = Isc$. At *Mpp*, maximum power can be drawn from PV module. Plots for P – V and I -V can be seen in figure 2.3 (a) and 2.3 (b).

$$I = Iph\ Npp\ -\ Ir\ Npp\{exp\ (\frac{q(V - IRs\frac{Nss}{Npp})}{akTNs\ Nss})\ -\ 1\}\ -\ \frac{V - IRs\frac{Nss}{Npp}}{Rp\frac{Nss}{Npp}} \quad (2.1)$$

$$I = Iph\ -\ Ir\ \{exp\ (\frac{q(V - IRs)}{akTNs})\ -\ 1\}\ -\ \frac{V - IRs}{Rp} \quad (2.2)$$

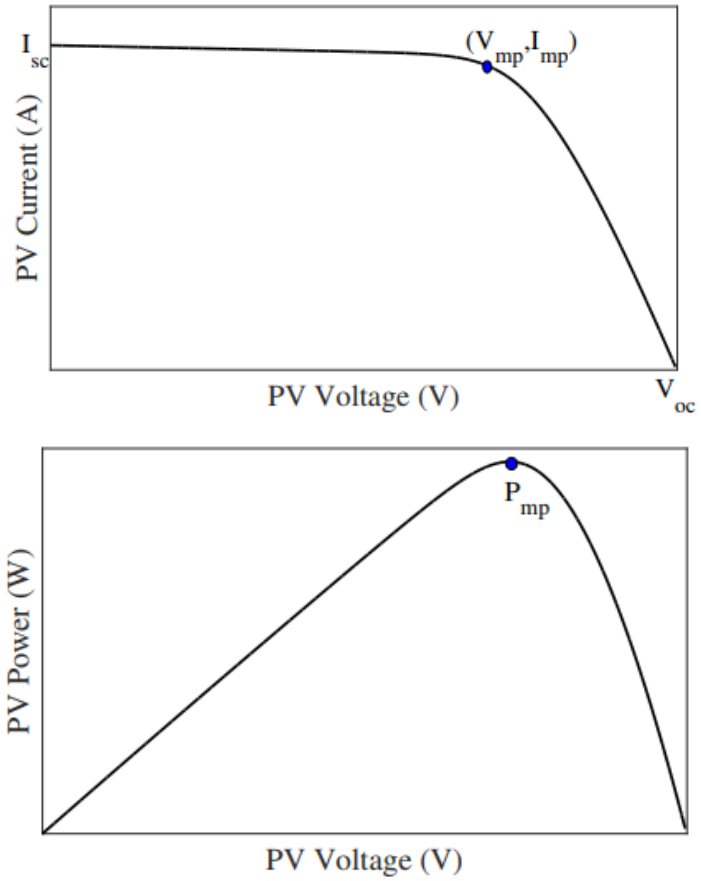

Figure 2.3(a) *I – V characteristics, 2.2(b) P -V characteristics of PV module*

In equation 2.2, The output voltage (V) of the PV module and the output current (I) of the PV module are denoted by V and I, respectively, while k represents the Boltzmann constant and q represents the charge of an electron.

2.3.2 Mismatching conditions

Mismatching conditions in solar PV systems occur when the electrical characteristics of the photovoltaic modules are not uniform or

well-matched. These conditions can arise from various factors such as manufacturing variations, aging differences, shading, soiling, or module damage [10]. The presence of mismatched modules can have significant consequences for the performance and power output of the solar PV system. In a series-connected configuration, the weakest module sets the limit for current flow, reducing the overall system performance. In a parallel-connected configuration, voltage differences among the modules lead to imbalanced currents and decreased power output.

To address mismatching conditions, a new approach has been discussed in [11]. These include carefully selecting and grouping modules with similar characteristics, performing regular maintenance to minimize shading and soiling, and utilizing bypass diodes to mitigate shading effects. Advanced techniques like maximum power point tracking (MPPT) algorithms can optimize power output by continuously adjusting the operating point of each module based on its characteristics. Addressing mismatching conditions is crucial for maximizing the efficiency and reliability of solar PV systems.

2.4 MPPT concept and types

The ability to extract the maximum power from a PV source is influenced by various factors, including irradiance (G), temperature (T). The concept of maximum power point tracking (MPPT) aims to align the operating point of the PV array with the power converter to achieve maximum power output. To achieve this, the effective resistance of the PV module is adjusted to match the resistance at the maximum power point [12]. However, due to changing environmental conditions and nonlinear characteristics, tracking the MPP presents challenges.

The I-V characteristics of a photovoltaic (PV) system demonstrate a maximum power point tracking under uniform irradiance conditions. However, this optimal point varies with changes in G and T, requiring the development of maximum power point tracking (MPPT) algorithms capable of accurately capturing the maximum power under diverse atmospheric conditions [27]. In situations where mismatching conditions occur, resulting in multiple peaks in the P-V curve, different methods have

been proposed to effectively track the maximum power. These methods vary in terms of their flexibility, cost, speed, and complexity of implementation. A proficient MPPT algorithm should demonstrate high precision, quick tracking speed, low complexity, minimal sensor dependencies, the capability to track the global peak with minimized oscillations.

Various MPPT algorithms have been discussed for tracking Maximum Power such as Perturb and Observe [13] where step size is considered for tracking time. Larger the step size, less time will be taken to track. A Table II is drawn for conclusion for change in perturbation with respect to change in power

TABLE II. PERTUBATION TABLE FOR P &O

Perturbation(old)	**ΔP**	**Perturbation(new)**
+ve	**+ve**	**-ve**
+ve	**-ve**	**+ve**
-ve	**+ve**	**+ve**
-ve	**-ve**	**-ve**

Incremental conductance involves the study the slope on PV curve at MPP point.

$$\frac{\mathrm{dP}}{\mathrm{dV}} = 0\ ;\ At\ MPP \tag{2.3}$$

$$\frac{\mathrm{dP}}{\mathrm{dV}} > 0\ ;\ At\ \text{Right of}\ MPP \tag{2.4}$$

$$\frac{\mathrm{dP}}{\mathrm{dV}} < 0\ ;\ At\ \text{Left of}\ MPP \tag{2.5}$$

$$\frac{\mathrm{dP}}{\mathrm{dV}} = \frac{\mathrm{d(IV)}}{\mathrm{dV}} = \mathrm{I} + \mathrm{V}\frac{\mathrm{dI}}{\mathrm{dV}} \cong \mathrm{I} + \mathrm{V}\frac{\Delta \mathrm{P}}{\Delta \mathrm{V}} = 0 \tag{2.6}$$

In [14], Incremental conductance with sliding mode control have been discussed which comes under the perturbation techniques. Methods such as Artificial Techniques which involves Artificial Neural Network [15] and Fuzzy logic [16][17] are more AI based which has faster tracking speed, higher accuracy but has higher complexity. For populated search space, Particle Swarm Optimization is preferred, where a collection of particles, also referred to as individuals, is utilized. Each particle represents a candidate solution. The particles mimic the success of their

neighboring particles while aiming to achieve their own success. The movement of each particle is guided by the performance of the most successful particle in the entire system. Additionally, the particle's position is established according to the optimal solution found by that particular particle. This calculation is carried out according to the equation (2.7).

$$x_i^{k+1} = x_i^k + v_i^{k+1} \quad (2.7)$$

The velocity component, represented by vi, indicates the step size. Equation (2.8) provides the expression for calculating this velocity component

$$v_i^{k+1} = wv_i^{k+1} + c_1 r_1\{P_{best,i} - x_i^k\} - c_2 r_2\{G_{best,} - x_i^k\} \quad (2.8)$$

The acceleration coefficients, *c1* and *c2*, along with the inertia weight, w, play a crucial role in this algorithm. Random numbers, *r1* and *r2*, within the range of 0 and 1, are utilized in the calculations. The personal best of each particle, $P_{best,i}$ and the best particle in the entire system, $G_{best,i}$ contribute to the determination of particle positions. A smaller value of w amplifies the particle's ability to explore local solutions, whereas a larger value of w accelerates the search for global solutions.

In a study mentioned in [18], an improved PSO algorithm is proposed that incorporates an exponential parameter control technique is employed to improve the performance of the traditional PSO algorithm. Another research [19] introduces a PSO algorithm that integrates a window-based search technique, which aims to minimize the search space and improve the convergence speed of the algorithm. Moreover, it addresses power oscillations during the transient phase. The paper also presents an algorithm specifically designed to distinguish between uniform and mismatching conditions in a solar PV system.

2.5 Conclusion

The study done for the PV system connected with a boost converter with the application of different MPPT technique studied are presented in this chapter is presented in “Investigation of various Global peak tracking algorithms” in detail. The literature review is studied to analyze design of boost converter along with the studies done on various tracking algorithms

their advantages and disadvantages. Among various MPPT techniques discussed, PSO provides fastest tracking time and is more suitable for global peak tracking for non-uniform shading. In the next chapters, design of boost converter with its modelling along with 3 Global peak tracking techniques along with conventional P&O are discussed.

CHAPTER 3

DESIGN OF SOLAR PV AND BOOST CONVERTER

3.1 Introduction

In this chapter, study of Solar PV characteristics and its current equations are been presented along with the characteristics of effect of changes in environmental variations. Further, the Design of Boost converter modes have been studied. Modelling of practical boost converter using Small Signal modelling and the effect of change in duty ratio on current and voltage have been discussed using Frequency Response Analysis. The values for the components of boost converter are evaluated for different duty cycles and final value are decided from the conclusion based on the values obtained.

3.2 Modeling of Solar PV

The modelling of solar PV systems is a critical aspect that involves creating mathematical and computational models to understand how these systems behave, perform, and interact with their environment [10]. These models capture the electrical, thermal, and optical characteristics of the system, enabling analysis, design, and optimization.

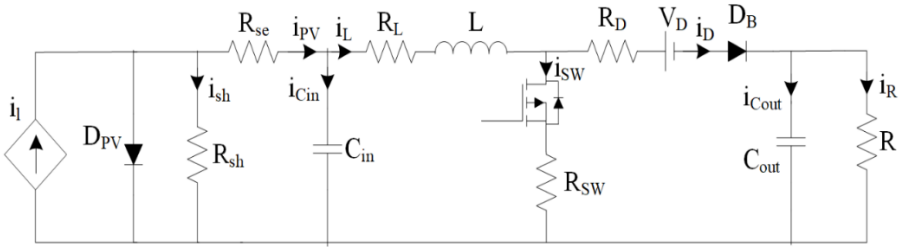

Fig 3.1. *Electrical Model of Solar PV*

Solar PV system modelling includes various components such as the PV array, power electronics, energy storage, and control systems. Mathematical equations are used to represent the PV array, considering factors like irradiance and temperature, series and parallel connections, and shading effects. Power electronics components like inverters and

converters are also modelled to understand their electrical behaviour and control mechanisms. The work utilized the equivalent circuit presented in [5] that is depicted in Fig. 3.1. A model of PV array consisting a dependent current source I_{ph} which depends on irradiance, anti-parallel diode, MOSEFT switch with a body diode, input and output capacitor, inductor and resistor load as shown in figure 3.1.

The equation for the PV current can be represented as,

$$I = I_{ph} - I_s \left(exp\frac{q(V+R_sI)}{aKTN_s} - 1\right) - \frac{(V+IR_s)}{R_s} \quad (3.1)$$

Where I_{ph} (3.1) is defined as [2],

$$I_{ph} = (I_{sc} + K_i(T - 298.5))\frac{G}{1000} \quad (3.2)$$

And, I_s (3.3) is written as [2],

$$I_s = \frac{I_{sc} + K_i(T-298.15)}{exp(q((V_{oc}+K_v(T-298.15))/aKTN_s))-1} \quad (3.3)$$

The changes in environment factors can alter the power characteristics. `These factors can be as follows:

A) Effect of Solar Irradiation

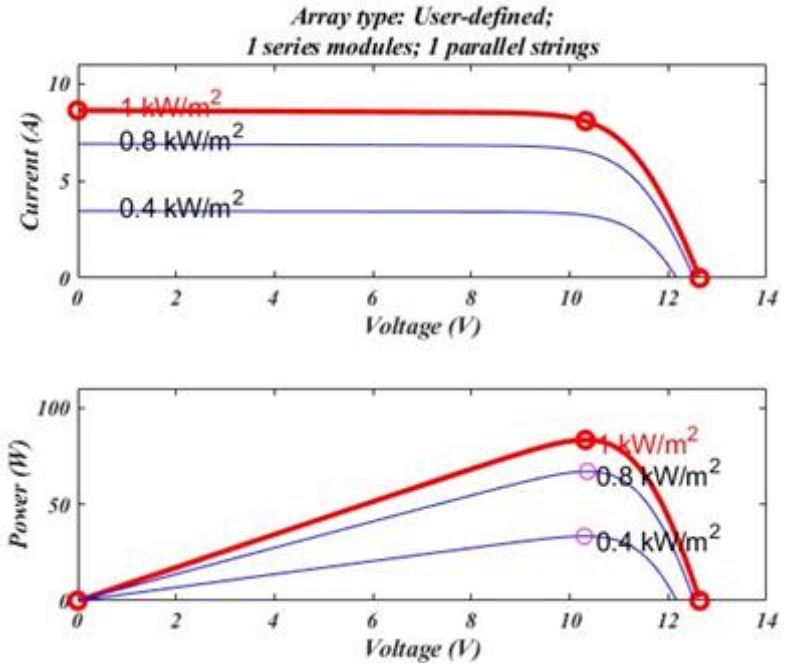

Fig 3.2*. Effect of Solar irradiation on I - V and P – V curve*

Figure 3.2 shows the Effect of Solar irradiation on *I - V* and *P – V* curve. The *I -V* curve, which illustrates the electrical behaviour of the PV module under various conditions, is directly affected by changes in solar irradiation levels. As solar irradiation intensifies, more photons interact

with the PV module, leading to an increased generation of electron-hole pairs within the semiconductor material. This results in a higher photocurrent flowing through the PV module. Consequently, the *I* - *V* curve shifts upward, indicating a rise in the current output of the PV system. Moreover, solar irradiation also impacts the open-circuit voltage (V_{oc}) and the maximum power point voltage (V_{mpp}) of the PV system. V_{oc} represents the voltage across the PV module when no current is present and is influenced by the energy of the incident photons. With higher solar irradiation, more energetic photons are absorbed, leading to an increase in V_{oc}. Similarly, V_{mpp}, which represents the voltage at which the PV system operates at maximum power output, is also influenced by solar irradiation. As the incident irradiation increases, the V_{mpp} of the *I* - *V* curve shifts towards higher voltages, indicating an elevation in the optimal operating point of the PV system. A small change in irradiation pattern can bring around 2-5V difference in voltage and consequently current changes.

B) Effect of Temperature Variation

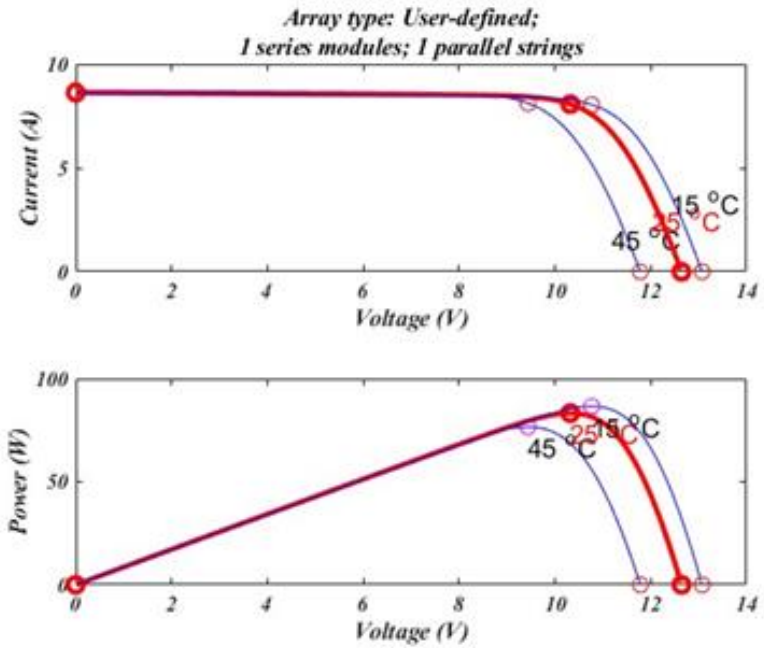

Fig 3.3*. Effect of Temperature variation on I - V and P – V curve*

Fig 3.3 represents *I* -*V* and *P* – *V* curve under change in Temperature. Changes in temperature can significantly impact the electrical performance and efficiency of PV modules. The effect of temperature variation is particularly evident in the current output of the PV system. As

temperature rises, the internal resistance of the PV module tends to decrease, resulting in an increase in current. Conversely, as temperature drops, the internal resistance increases, leading to a decrease in current. This behaviour is clearly observed in the IV curve, where current decreases with rising temperature and increases with decreasing temperature.

Temperature variation also affects the voltage characteristics of the PV system, specifically the open-circuit voltage (V_{oc}). V_{oc} shows an inverse relationship with temperature, decreasing as temperature rises and increasing as temperature drops. This phenomenon is reflected in the I - V curve, where voltage decreases with increasing temperature and increases with decreasing temperature.

Additionally, temperature fluctuations have an impact on the maximum power point (MPP) of the PV system. The MPP represents the voltage and current combination at which the PV system operates with maximum power output. With increasing temperature, the MPP voltage tends to decrease, resulting in a lower power output. Conversely, decreasing temperature leads to an increase in MPP voltage and higher power output. These variations are depicted in the PV curve, where the MPP voltage shifts downward with rising temperature and upward with decreasing temperature

C) Effect of Partial Shading

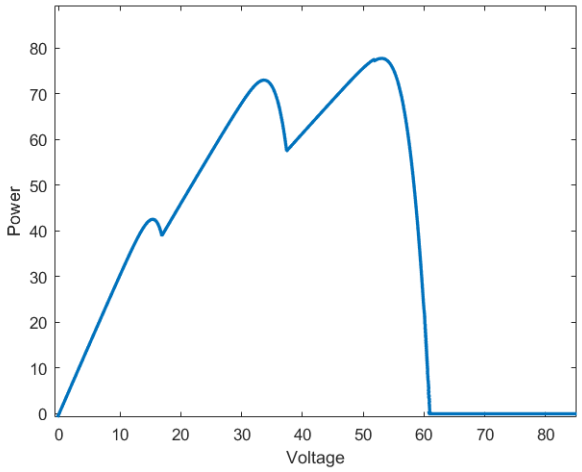

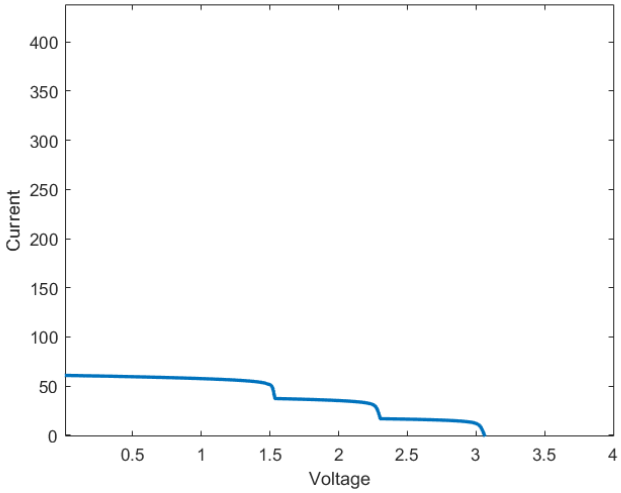

***Fig 3.4**. a) P – V plot b) I -V plot for solar PV due to partial shading*

Fig 3.4 (a), (b) shows P – V and I – V characteristics of Solar PV in case of partial shading Partial shading has a notable impact on the operation of solar photovoltaic (PV) systems. When certain sections of a PV module or array are shaded, it creates an uneven distribution of sunlight across the system. This shading can be caused by factors like nearby buildings, trees, or other obstructions. The consequences of partial shading on a solar PV system are twofold. Firstly, it results in a decrease in the amount of solar irradiation reaching the shaded areas. As a result, the shaded PV cells or modules receive less sunlight and generate less electricity, leading to a reduction in the overall power output of the system. Secondly, partial shading can create a mismatch in operating conditions between shaded and unshaded cells or modules within the PV array. This mismatch causes a phenomenon known as the "partial shading effect" or "multiple peaks effect." Instead of the typical single peak associated with uniform illumination, the IV curve of the system exhibits multiple peaks. Partial shading has a considerable role in determining the output power. When irradiation received on a PV panel i.e. shaded cells is different to irradiation received on the unshaded cells, then $I_{unshaded} > I_{shaded}$. Then, this mismatch turns shaded cells to act as a sink. This power loss in the shaded cells leads to hot spot effect [6]. In order to bridle the issue, bypass diodes are connected in anti-parallel with PV sub-module. To simulate the effect of shading, the string having four modules in series along with bypass diode in parallel is considered. Under uniform irradiation, the bypass

diodes do not operate as it is reverse biased. Bypass diode gets forward biased under partial shading conditions and irradiated cells will engage in generating power [2].

The partial shading effect causes a complex behavior in the IV curve, where different local maximum power points (MPPs) exist. Traditional maximum power point tracking (MPPT) algorithms may struggle to accurately track the global MPP due to the presence of shaded and unshaded areas operating at different voltage levels.

3.3 Modelling of Ideal Boost converter

The modeling of a boost converter is an essential step in understanding its behavior and characteristics. By developing accurate mathematical equations and circuit models, engineers can gain valuable insights into the converter's performance under different conditions. The process begins with assuming ideal conditions, where all components and switching operations are considered perfect. However, practical considerations are also taken into account by incorporating non-idealities such as resistances, voltage drops, and switching losses. These non-idealities have a significant impact on the converter's efficiency and overall performance. By simulating the boost converter using tools like SPICE or MATLAB/Simulink, engineers can assess its behavior, analyze the effects of non-idealities, and optimize its design. The small signal analysis is used to derive the transfer functions of the boost converter as follows:

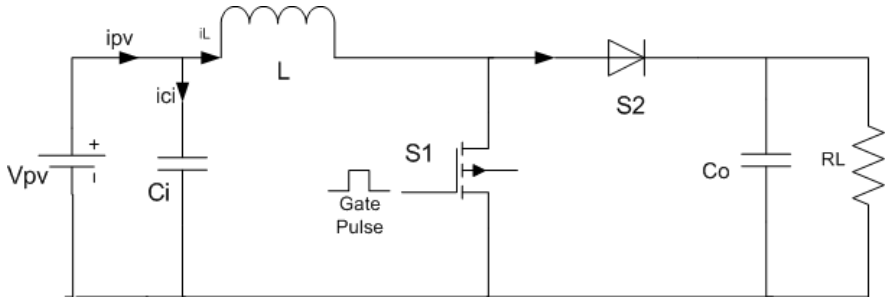

***Fig 3.5**. Schematic diagram of ideal boost converter with Input and Output capacitor*

***Mode 1*:** the switch S_1 is turned ON. Source *Vpv* is attached to the circuit with switch closed and *Ipv* current flows. During this mode the energy is stored in the inductance *L*, and the *Ipv* current gradually increases. The diode *S2* is in OFF state. Two voltages, namely the source voltage and

inductor voltage, will be present at the output. Additionally, there will be additional voltages on the output side. Similarly, as the current flows through the capacitor, it results in the charging of the capacitor. Therefore, the modeling can be accomplished using the concept of state space modeling. The first step involves formulating the equations that describe the system's behavior, considering variables such as the inductor current (i_L) and the photovoltaic voltage (V_{pv}). These equations capture the dynamics and relationships within the system. Subsequently, the averaging of these equations is performed, and the transfer function for the control parameters, namely the duty cycle (d) and photovoltaic voltages (V_{PV}), is derived. In this study, the state variables i_L and V_{PV} are utilized, and V_{PV} is identified as the output variable. Fig 3.6 shows the Boost converter in ON state.

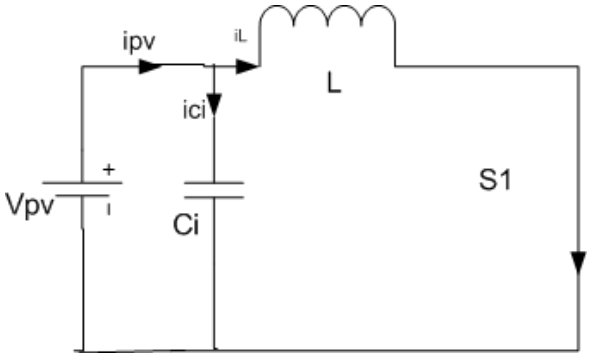

Fig 3.6*. Schematic diagram of ideal boost converter in ON state*

The State Space modelling is done as the inductor equation in written as,

$$i_L = i_{PV} - i_{Ci} \tag{3.4}$$

$$C_i = \frac{dV_{pv}}{dt} = -\frac{V_{pv}}{R_{pv}} - i_L \tag{3.5}$$

The -ve sig represents that the load is a source and Ri is the source Resistance.

$$V_{PV} = -\frac{V_{PV}}{C_i R_{pv}} - \frac{i_L}{C_i} \tag{3.6}$$

$$L\frac{di_L}{dt} = V_{PV} \text{ (From KVL)} \tag{3.7}$$

$$i_L = \frac{1}{L} V_{PV} \tag{3.8}$$

$$\begin{matrix} \dot{i_L} \\ \dot{v_{pv}} \end{matrix} = \begin{bmatrix} 0 & \frac{1}{L} \\ -\frac{1}{C_i} & -\frac{1}{C_i R_{pv}} \end{bmatrix} \begin{bmatrix} i_L \\ v_{PV} \end{bmatrix} + \begin{bmatrix} 0 \\ 0 \end{bmatrix} v_o \tag{3.9}$$

Mode 2: When the switch is turned off, the current changes its path to flow through the diode. This causes a reverse current to flow in the inductor, resulting in the presence of two currents: Ipv and Ici. At this point, the inductor current (iL) can follow two different routes. One portion of the current (ico) passes through the output capacitor (co), while the remaining portion (Io) flows through the load resistor (RL) as illustrated in Figure 3.7

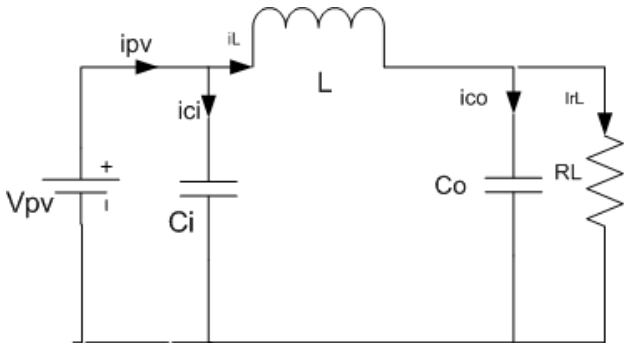

Fig 3.7*. Schematic diagram of ideal boost converter in OFF state*

$$\cdot i_L = i_{PV} + i_{Ci} \quad (3.10)$$

$$\frac{dV_{pv}}{dt} = -\frac{V_{pv}}{C_i R_{\text{pv}}} - \frac{V_{PV}}{C_i R_{\text{pv}}} \quad (3.11)$$

The -ve sig represents that the load is a source and Ri is the source Resistance.

$$V_{PV} = -\frac{V_{PV}}{C_i R_{\text{pv}}} - \frac{i_L}{C_i} \quad (3.12)$$

$$L\frac{di_L}{dt} = V_{PV} - V_o \text{ (From KVL)} \quad (3.13)$$

$$i_L = \frac{1}{L}V_{PV} - \frac{V_o}{L} \quad (3.14)$$

From equations (3.13) and (3.14)

$$\begin{matrix} \dot{i_L} \\ \dot{v_{pv}} \end{matrix} = \begin{bmatrix} 0 & \frac{1}{L} \\ -\frac{1}{C_i} & -\frac{1}{C_i R_{\text{pv}}} \end{bmatrix} \begin{bmatrix} i_L \\ v_{PV} \end{bmatrix} + \begin{bmatrix} -\frac{1}{L} \\ 0 \end{bmatrix} v_o \quad (3.15)$$

$$\bar{\text{A}} = \text{A}_1\text{d} + \text{A}_2(1\text{-d}) \quad (3.16)$$

$$\bar{A} = \begin{bmatrix} 0 & \frac{1}{L} \\ -\frac{1}{C_i} & -\frac{1}{C_i R_{\text{pv}}} \end{bmatrix} d + \begin{bmatrix} 0 & \frac{1}{L} \\ -\frac{1}{C_i} & -\frac{1}{C_i R_{\text{pv}}} \end{bmatrix} (1-d)$$

(3.17)

$$\bar{A} = \begin{bmatrix} 0 & \frac{1}{L} \\ -\frac{1}{C_i} & -\frac{1}{C_i R_{\text{pv}}} \end{bmatrix} \quad (3.18)$$

Similarly, to calculate B matrix

$$\bar{B} = B_1 d + B_2(1\text{-}d)` \quad (3.19)$$

$$\bar{B} = \begin{bmatrix} 0 \\ 0 \end{bmatrix} d + \begin{bmatrix} -\frac{1}{L} \\ 0 \end{bmatrix} (1\text{-}d) \quad (3.20)$$

$$\begin{matrix} \dot{\imath_L} \\ \dot{v_{pv}} \end{matrix} = \begin{bmatrix} 0 & \frac{1}{L} \\ -\frac{1}{C_i} & -\frac{1}{C_i R_{\text{pv}}} \end{bmatrix} \begin{bmatrix} i_L \\ v_{PV} \end{bmatrix} + \begin{bmatrix} -\frac{-(1-d)}{L} \\ 0 \end{bmatrix} v_o \quad (3.21)$$

(3.20) and (3.21) can be written as,

$$\dot{\imath_L} = \frac{1}{L} V_{PV} - \frac{(1-d)}{L} V_o \quad (3.22)$$

$$\dot{v_{pv}} = -\frac{1}{C_i} i_L - \frac{1}{C_i R_{\text{pv}}} V_{pv} \quad (3.23)$$

Introducing state variables,

$$i_L = I_L + \widehat{\imath_L}, v_o = V_o + \widehat{v_o}, d = D + \hat{d}, v_{pv} = V_{pv} + \widehat{v_{pv}} \quad (3.24)$$

$$L \frac{di_L}{dt} = V_{PV} - (1-d)V_o \quad (3.25)$$

$$L \frac{dI_L + \widehat{\imath_L}}{dt} = (V_{pv} + \widehat{v_{pv}}) - (1 - (D-d))(V_o + \widehat{v_{pv}}) \quad (3.26)$$

By equating the DC and AC quantities and focusing on AC quantities while disregarding second-order quantities, the analysis can be continued.

$$L \frac{d\widehat{\imath_L}}{dt} = \widehat{v_{PV}} - \hat{d}V_o - D\widehat{v_O} \quad (3.27)$$

Since, (1-D) $\widehat{v_o}$= 0;

$$L \frac{d\widehat{\imath_L}}{dt} = \widehat{v_{PV}} - \hat{d}V_o \quad (3.28)$$

$$\widehat{\dot{\imath_L}} = \frac{\widehat{v_{pv}}(s)}{s_L} + \frac{\hat{d}(s)}{s_L} V_o \quad (3.29)$$

From equation 3.30

$$c_i \frac{dV_{pv} + \widehat{v_{pv}}}{dt} = -(V_{pv} + \widehat{v_{pv}}) \frac{1}{R_{\text{pv}}} - (I_L - \widehat{\imath_L}) \quad (3.30)$$

$$c_i \frac{d\widehat{v_{pv}}}{dt} = -\widehat{v_{pv}} \frac{1}{R_{\text{pv}}} - (\widehat{\imath_L}) \quad (3.31)$$

Taking Laplace on both sides in 3.31, we get

$$sc_i \widehat{v_{pv}} = -\widehat{v_{pv}}(s) \frac{1}{R_{\text{pv}}} - (\widehat{\imath_L}) \quad (3.32)$$

Finally we get our transfer function as ($\frac{\widehat{v_{pv}}}{d}$), control duty cycle ($d$) to Photovoltaic voltage (v_{PV})

$$\frac{\widehat{v_{pv}}}{d} = \frac{V_o}{s^2 LC_i + \frac{s_L}{R\text{pv}} + 1} \tag{3.33}$$

By Substituting v_{pv} in equation 3.29 from 3.32, we get transfer function as ($\frac{\widehat{i_{pv}}}{d}$), control duty cycle ($d$) to Photovoltaic Current (i_{pv})

$$\frac{\widehat{i_{pv}}}{d} = \frac{V_o(sC_i + \frac{1}{R\text{pv}})}{s^2 LC_i + \frac{s_L}{R\text{pv}} + 1} \tag{3.34}$$

Also, we know,

$$R_{\text{pv}} = (1 - D)^2 R_L \tag{3.35}$$

The value of transfer function in equation (3.33) and (3.34) is calculated for different duty cycle d at 0.3, 0.4, 0.5, 0.6 respectively to arrive at the point to check the stability of the converter i.e. up to what value of d can converter remain stable.

A) At d=0.3

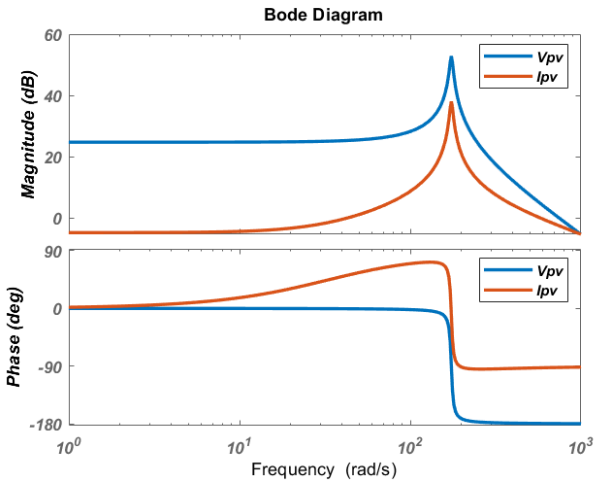

B) At d=0.4

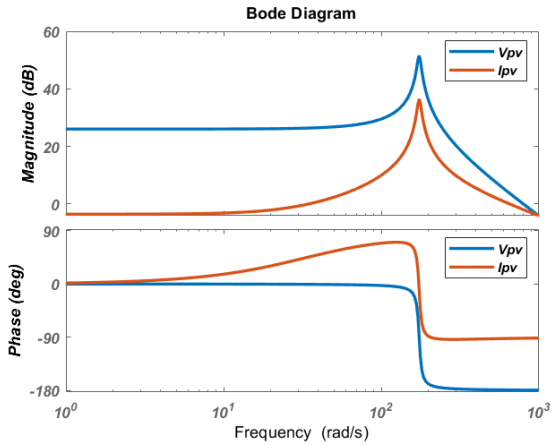

C) At d=0.5

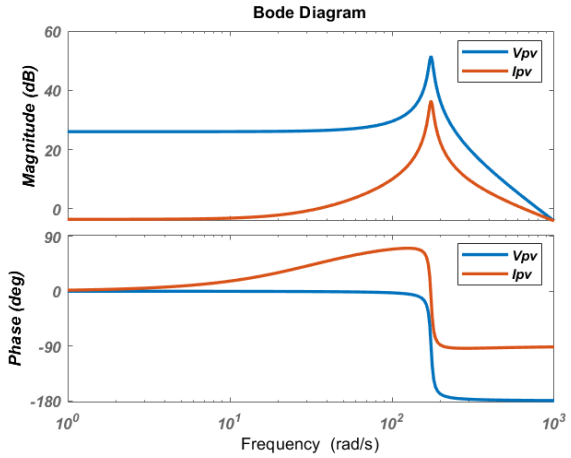

D) At d=0.6

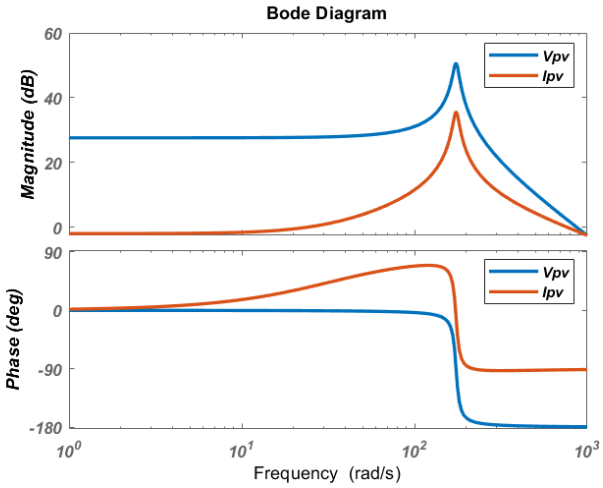

E) At d=0.7

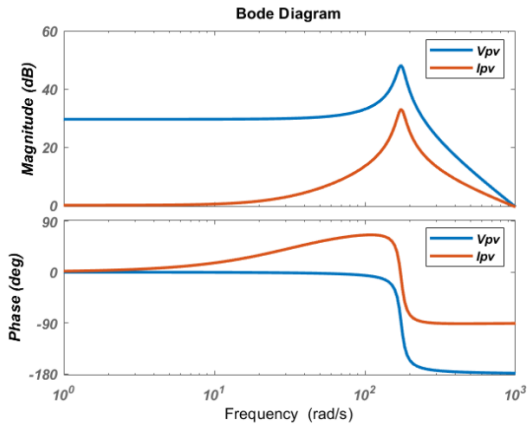

***Fig 3.8**. Bode plots for $\frac{\widehat{v_{pv}}}{d}$, $\frac{\widehat{i_{pv}}}{d}$ for a) 0.3, b) 0.4, c) 0.5, d) 0.6, e) 0.7*

Finally, we obtain the transfer function for Frequency response analysis to check for stability. Conventionally, we can also approach towards the Circuit Averaging method shown in fig 3.8 to derive the transfer functions as addition of components like ESR of inductance and Capacitance is easy for derivation purpose and we can get solutions for different transfer functions. So, fir the Ideal Boost converter scenario, Small Signal Transfer Functions are derived from the circuit model as shown in Fig 3.9

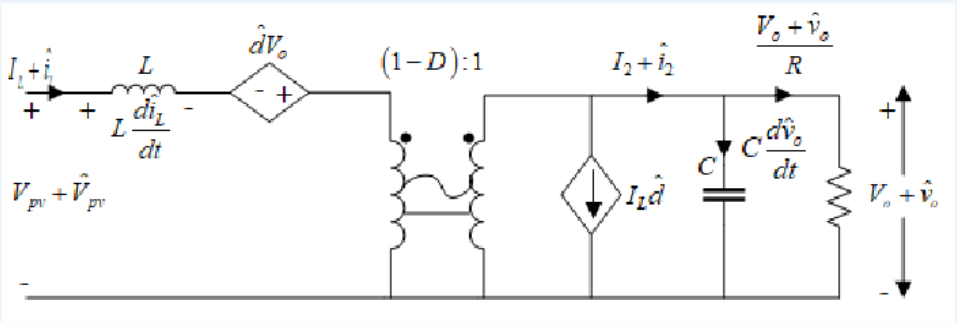

***Fig 3.9** Circuit Diagram for Boost converter using Circuit Averaging*

Here $R = R_L$, $C = C_o$ from previous derivation. Dependent sources are removed in DC analysis; Hence, we can calculate G_{vd} i.e. control duty to output transfer function as

$$G_{vd} = \left.\frac{\widehat{v_o}}{\hat{d}}\right|_{\widehat{v_{pv}}=0,\widehat{i_o}=0} = \frac{1}{D'} x \frac{\frac{R}{(1+sRC)}}{\left[\frac{sL}{D'}+\frac{R}{(1+sRC)}\right]} x \left\{V_o - \frac{I_L}{D'} sL\right\} \quad (3.36)$$

$$G_{vd} = \frac{V_{pv}\left\{1-\frac{sL}{RD'^2}\right\}}{\left[\frac{sL}{R}+D'^2+s^2LC\right]} \quad (3.37)$$

Equation (3.37) has 2 poles and it is LOAD dependent and one zero lies on right half of the s -plane. Frequency analysis response for

$G_{vd}$is shown in Fig 3.10

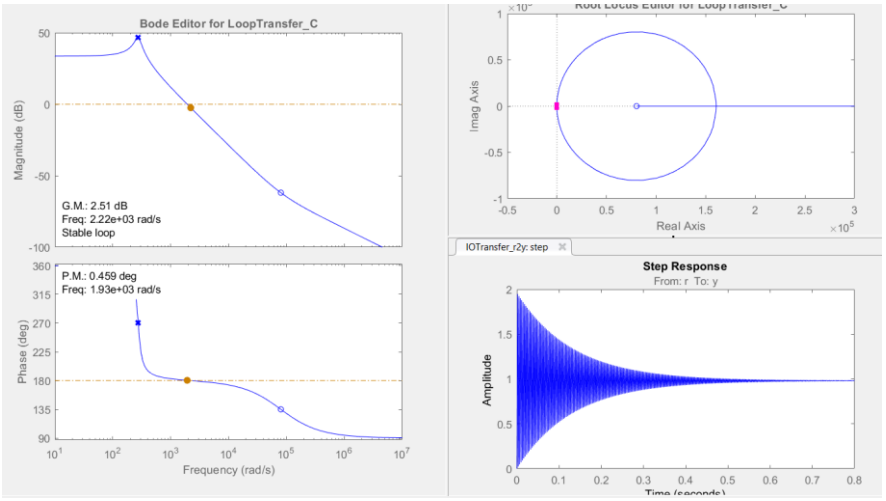

***Fig 3**.10 Bode plot and time response analysis for G_{vd}(s)*

Similarly, for G_{vg}, We can calculate its Transfer function as,

$$G_{vg} = \left.\frac{\widehat{v_o}}{\widehat{v_{pv}}}\right|_{\hat{d}=0,\widehat{i_o}=0} = \frac{1}{D'}\frac{\frac{R}{(1+sRC)}}{\left[\frac{sL}{D'}+\frac{R}{(1+sRC)}\right]} \qquad (3.38)$$

Equation (3.38) can be finally written as,

$$G_{vg} = \frac{D'^2}{\left[\frac{sL}{R}+D'^2+s^2LC\right]} \qquad (3.39)$$

Frequency analysis response for G_{vg} for d =0.5 is shown as in Fig 3.11

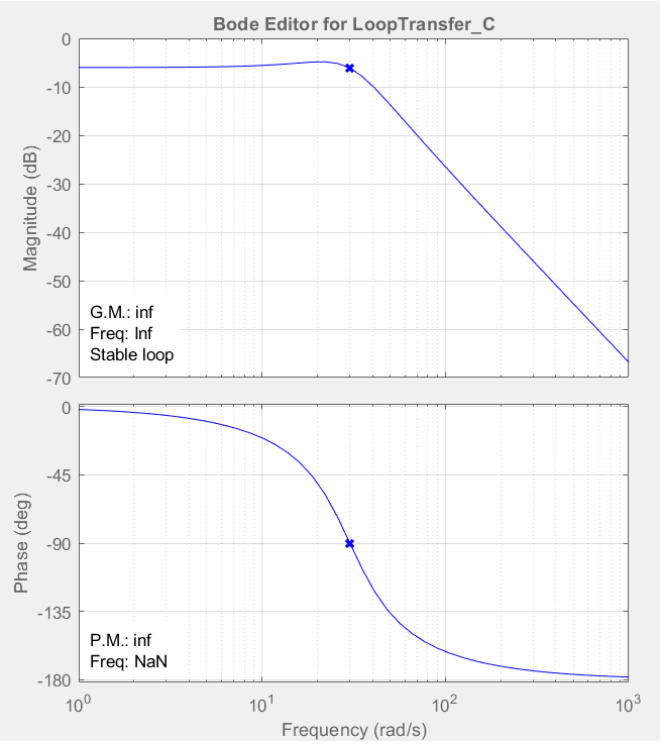

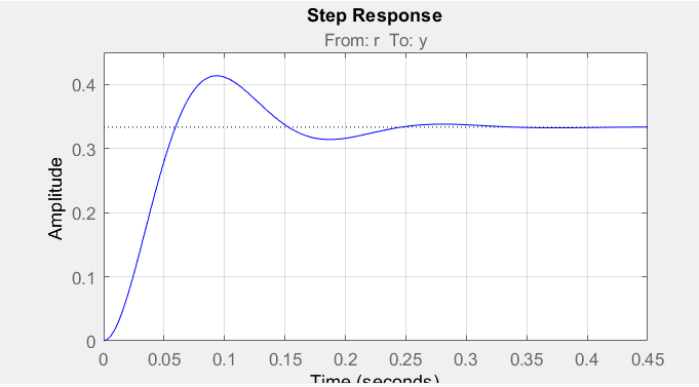

***Fig 3**.11 Bode plot and time response analysis for $G_{vg}(s)$*

By analyzing the Bode plot, all the poles and zeros of the transfer function are located in the left half-plane of the complex plane, it signifies the stability of the system. This implies that the boost converter will demonstrate stable and consistent performance across various duty cycle values. Conversely, for any poles or zeros are situated in the right half of the Bode plot, it indicates the possibility of instability in the boost converter. Unstable behaviour can result in oscillations, excessive ripple, or even failure of the system. So, for different values of duty ration the system is found to be stable.

3.4 Modelling of Practical Boost converter

The practical boost converter consists of key elements working in tandem to accomplish the voltage boosting process. The PV panels, as the primary energy source, generate DC voltage when exposed to sunlight. the ESR of capacitors and inductors is an important parameter to consider in practical boost converters for solar PV systems.

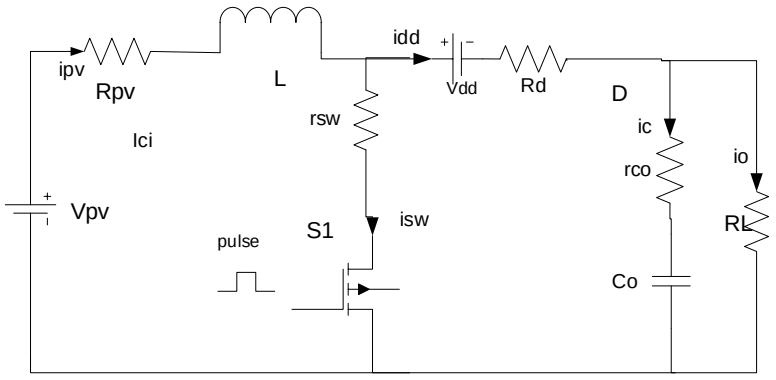

***Fig 3.12** Schematic diagram of Practical Boost converter with ESR*

Fig 3.12 shows the diagram of practical boost converter. By

accounting for the ESR, designers can ensure optimal performance, reduced power losses, and stable operation of the converter. An inductor is incorporated with an ESR (Equivalent Series Resistance) to store energy during the ON state of the switch and release it during the OFF state, regulating current flow and smoothing voltage ripples. ESR of the inductor influences the current ripple and the converter's ability to maintain a smooth and regulated output voltage. The switch, commonly a power MOSFET or an IGBT, controls the current flow within the boost converter by rapidly switching ON and OFF, thus managing energy transfer from input to output. A diode acts as a one-way valve, enabling current flow in a single direction and providing a path for the inductor current during the switch's OFF state. A capacitor with a ESR value, connected in parallel to the load, aids in stabilizing and filtering the output voltage, ensuring a consistent and steady DC voltage.

During operation, the switch allows energy storage in the inductor and current flow through the PV panels when ON. When OFF, the inductor's stored energy is transferred to the output through the diode, resulting in an increased output voltage surpassing the input voltage. The small signal modelling is performed just same as for the Ideal boost converter. Similarly, for the practical Boost converter, the transfer function can be derived as

$$G_{vd} = \left.\frac{\widehat{v_o}}{\hat{d}}\right|_{\widehat{v_{pv}}=0,\widehat{i_o}=0} \tag{3.40}$$

$$G_{vd} = \frac{(1+sC_o r_{co})(1\text{-}D)}{s^2LC_x+sC_OC_XR_X+R_LL+C_Or_{co}(1\text{-}D)^2+R_LR_x+(1\text{-}D)^2} \tag{3.41}$$

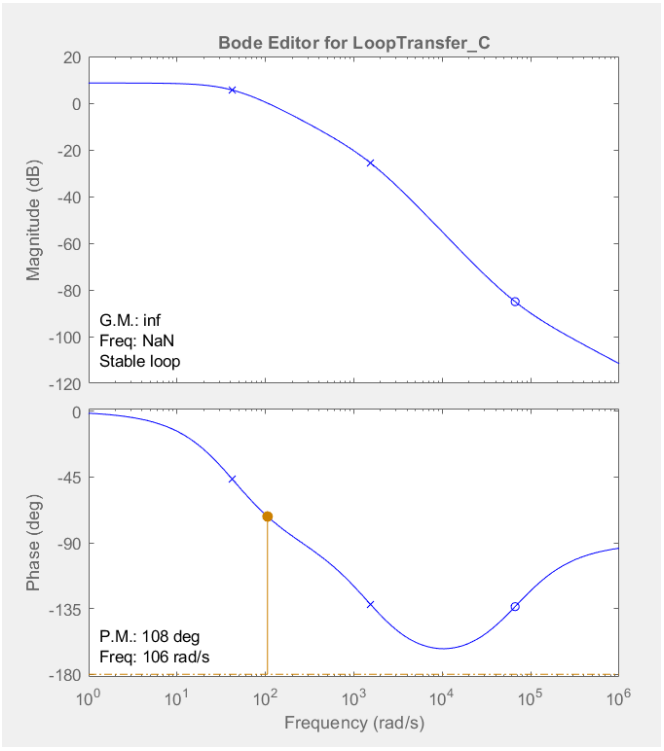

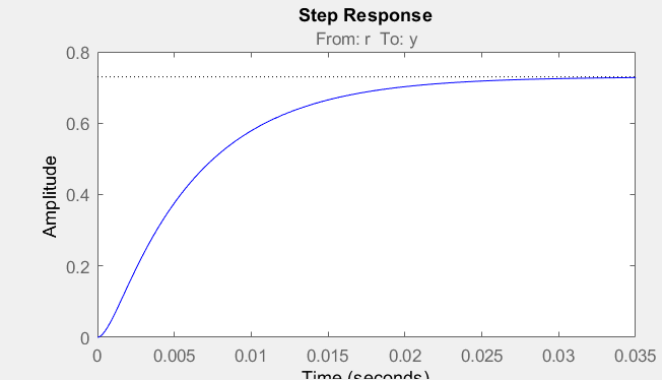

Fig 3.13 *Bode and Time response plot for $G_{vg}(s)$ at d =0.5*

Similarly, G_{vg}(s) is derived, and transfer function is as follows

$$G_{vg} = \left.\frac{\widehat{v_o}}{\widehat{v_{pv}}}\right|_{\hat{d}=0,\widehat{i_o}=0} \tag{3.42}$$

$$G_{vg} = \frac{(1+sC_o r_{co})(1-D)(-I_L)(r_{sw}-R_d)+V_{dd}+V_o-\frac{I_L(sL+R_x)}{(1-D)}}{s^2LC_x+sC_OC_XR_X+R_LL+C_Or_{co}(1-D)^2+R_LR_x+(1-D)^2} \tag{3.43}$$

Where,

$$V_o = \frac{V_{pv}-V_{dd}(1-D)^2}{R_LR_x+(1-D)^2} \tag{3.44}$$

$$I_L = \frac{V_{pv}-V_{dd}(1-D)R_L}{R_LR_x+(1-D)^2} \tag{3.45}$$

$$R_x = D(r_{sw} - R_D) + R_L + R_D \tag{3.46}$$

$$C_x = C_o(1 + R_L r_{CO}) \tag{3.47}$$

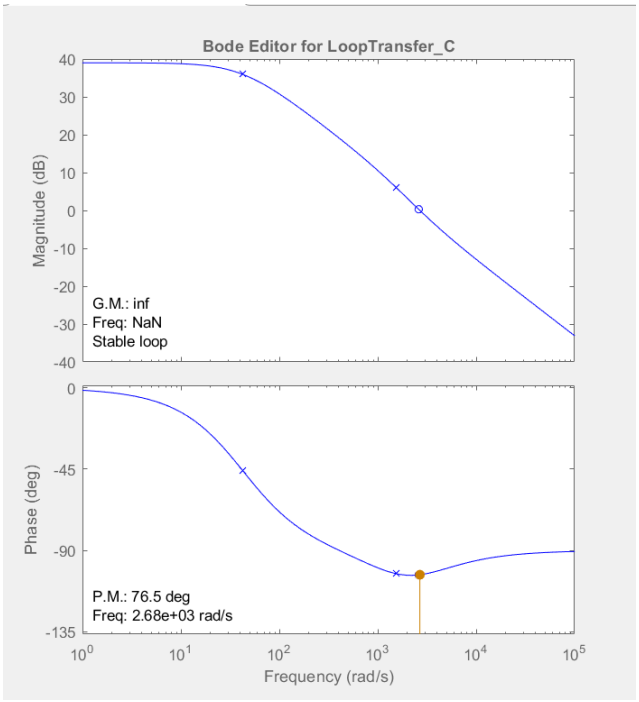

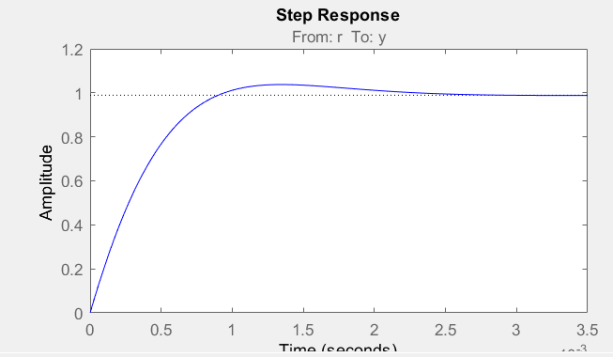

Fig 3.14 *Bode plot for $G_{vd}(s)$ at d =0.5*

The following Results shown above shows that the Frequency and Time response for the transfer function at d=0.5 is plotted. The bode plots shows that PM and GM are positive, hence the system is stable for d=0.5. In our previous investigations in Ideal case, we have drawn a conclusion that above d = 0.8, system goes into instability and gain drastically increases. Thus, it can be concluded for the system to perform efficiently, the voltage gain should be low in case of practical converter as shown in [28]. For small duty ratio, the converter works efficiently giving maximum performance with minimum losses.

3.5 Boost converter parameter calculation for solar PV

The DC/DC boost converter [3] requires four components for its operation: inductor, electronic switch like MOSFET or IGBT, a diode, output capacitor, and an input capacitor. In general, the converter can be

employed in the two modes. One known to be as Discontinuous Conduction Mode (DCM), responsible for low power operation and other as Continuous Conduction Mode (CCM) responsible for efficient power conversion. These modes depend on its switching period and energy storing capacity. However, for safe operation, it is generally recommended to operate boost converter in CCM mode only.

1. *Selection of Inductor value*

The large value of inductance increases the time constant while with the small value of inductance the converter goes into DCM. The boost inductor value is optimized to operate converter in the required range where we arrive at the concept of critical inductance [9].

$$L_{min} \geq \frac{R*(1-D)^2*D}{2*f_s} \tag{3.48}$$

From (1), L_{min} is defined as the minimum amount of inductance required to keep a continuous current. It plays a vital role in determining the performance of a converter. If $L>L_{min}$, then the converter operates in CCM, else it operates in DCM. f_s is the converter switching frequency. The value of the inductor computed is 3mH and its ESR is considered as 0.003 ohms.

2. *Selection of Input Capacitor*

To minimize the ripple in PV voltage, an input capacitor [6] is used to deliver current to the inductor with reduced ripple. The input current to capacitor is greater than zero, so the blue area in Fig. 3.15 is used to calculate the input capacitor value.

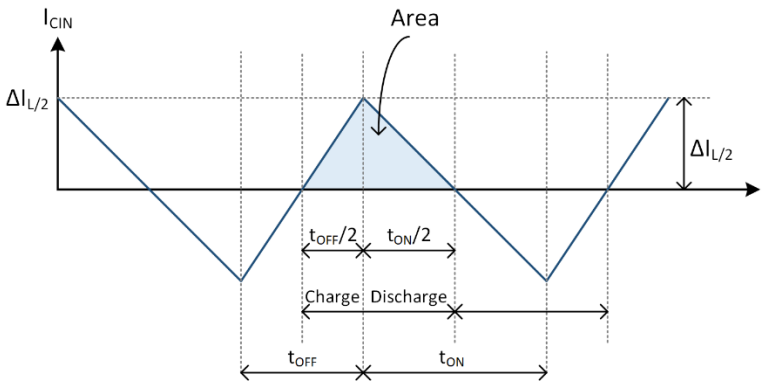

Fig 3.15*. Current waveform of C_{in}*

The PV voltage is given by (3.12).

$$\mathrm{I_{Cin}} = \mathrm{C_{in}} \frac{\Delta \mathrm{V}}{\Delta \mathrm{t}} \tag{3.49}$$

From (3.49), (3.50) is obtained,

$$\Delta V = I_{in} \frac{\Delta t}{C_{in}} \tag{3.50}$$

From Fig.3.12. ΔV is calculated using (3.50).

$$\Delta V = \frac{\Delta I_L}{8 * f_s * C_{in}} \tag{3.51}$$

$$C_{in} = \frac{\Delta I_L}{8 * f_s * \Delta V} \tag{3.52}$$

The current in the ripple inductor is defined as [9]:

$$\Delta I_L = \frac{V * D}{f_s * L} \tag{3.53}$$

Substituting (3.53) in (3.52), (3.54) is obtained.

$$C_{in} = \frac{V * D}{8 * {f_s}^2 * L * \Delta V} \tag{3.54}$$

where, C_{in} is input capacitance, V is PV voltage, f_s is the switching frequency of the converter, D is the duty ratio and L is the inductance. The value of C_{in} is calculated by (3.54), where ΔV is considered as 1% of input voltage. Hence, (3.54) can be written as in (3.55).

$$C_{in} \geq \frac{D}{8 * {f_s}^2 * L * 0.01} \tag{3.55}$$

3. Calculation of Output Capacitance

The value is chosen from ripples present in output voltage [9]. During the turn-on time, the output current can be written as is given by (3.56).

$$I_o = C_o \frac{\Delta V}{T_{ON}} \tag{3.56}$$

In (3.56), $\mathrm{T_{ON}}$ is substituted as $D * f_s$, Therefore,

$$C_O = \frac{D * I_o}{\Delta V_o * f_s} \tag{3.57}$$

For desired voltage ripple (say 1%), output capacitor can be written as:

$$C_O \geq \frac{D}{0.01 * f_s * R} \tag{3.58}$$

The load connected at the output, represented by R, is determined based on the output voltage and current. Using equation (3.58), the calculated capacitance value is 100µF, and an ESR (equivalent series resistance) value of 0.03 ohms is taken into account.

3.6 Conclusion

In this chapter, saw the small signal analysis for Ideal and Practical boost converter and derived the transfer function for the converter photovoltaic voltage to d and converter photovoltaic current to *d*. We saw the stability analysis checking frequency response analysis on different duty ratios. We observed that after duty ratio goes above 0.75 the converter goes out to stability as phase margin (PM) becomes negative.

As discussed in [10], The presence of the input capacitor and its equivalent series resistance (ESR) does not impact the stability of the system. Analysis using the Routh-Hurwitz criteria has confirmed that the system remains stable in an open-loop configuration, as all the poles and zeros are situated on the left half of the s-plane.

Thus, the Boost Converter parameters to be used in this work in shown in Table IV. PV Modules which are defined in Table III is considered for evaluation in this work. All three module with uniform irradiance at STC condition can generate the maximum power of 250 W. In the second experiment, multiple shading pattern consisting of Six PV modules with uniform irradiance at STC condition are simulated with different algorithms and it can generate the maximum power of 500 W.

TABLE III: CHARACTERISTICS OF USER DEFINED PANEL AT STC.

PV parameters	Variable	Value
Maximum power	P_{max}	83.2824 W
V/T. coefficient	V_{coeff}	-0.339% /° C
A/T. coefficient	I_{coeff}	0.063%/° C
Voltage at Max. power	V_{mp}	10.32 V
Current at Max. power	I_{mp}	8.07 A
Short Circuit Current	I_{sc}	8.62 A
Open Circuit Voltage	V_{oc}	12.304 V
Number of Cells in Series	N_s	20

TABLE IV: BOOST CONVERTER PARAMETERS FOR MPPT TRACKING

Parameter	Variable	Value
Inductor	L	3.3 mH
Inductor ESR	r_L	3 mΩ
Input Capacitor	*Cin*	100 µF
C_{in}, C_{out} ESR	r_c	0.03 Ω
Output Capacitor	*Cout*	100 µF

Load	*R*	30 Ω
MOSFET	*Vth*	5.7 mH
Internal Resistance	*Ron*	1 mΩ
Diode Knee voltage	*Vn*	0.7 V
Switching Frequency	*fs*	20kHZ

CHAPTER 4

GLOBAL MPPT TECHNIQUE AND ALGORITHMS

4.1 Introduction

In this chapter GMPPT algorithms are discussed. Global peak tracking algorithms play a crucial role in maximizing power extraction from photovoltaic (PV) systems. Among these algorithms, Particle Swarm Optimization (PSO), Hybrid Particle Swarm Optimization with Pattern Optimization (Hybrid POPSO), and conventional PSO have shown promise in achieving efficient power extraction. Extensive research has been conducted to evaluate their performance and effectiveness under various operating conditions. This chapter provides a comprehensive review and comparison of these algorithms, highlighting their strengths, limitations, and potential for future advancements.

4.2 Particle Swarm Optimization

The PSO algorithm [31] utilizes a population of particles to search for the optimal solution. Each particle represents a candidate solution and adjusts its position based on the success of neighboring particles. The particle's position is determined by considering both its personal best solution and the best solution found by the entire swarm. The update equation for the particle's velocity incorporates an inertia weight (*w*) that ensures a balance between local and global search. The value of *w* emphasizes local exploration, while a higher value promotes global exploration. By iteratively updating particle velocities and positions, PSO aims to converge towards the optimal solution. Here is an overview of the equations and steps involved in the PSO algorithm:

1. Initialization:
    - Initialize the population of particles with random positions and velocities.
    - Set the personal best position ($P_{best,}$) for each particle as its initial

position.

- Identify the global best position (G_{best}) among all the particles.

2. Update Particle Velocity:
    - Update the velocity of each particle using the following equation:

$$v_i^{k+1} = wv_i^{k+1} + c_1 r_1\{P_{best,i} - x_i^k\} - c_2 r_2\{G_{best,} - x_i^k\} \quad (4.1)$$

The updated velocity of particle *i*, denoted as $v_i^{k+1}\}$, is determined by various factors. These include the inertia weight (*w*), acceleration coefficients (c_1 and c_2), random numbers (r_1 and r_2), the personal best position of particle $P_{best,i}$, and the global best position G_{best} . Update Particle Position.

- Update the position of each particle using the following equation:

$$x_i^{k+1} = x_i^k + v_i^{k+1}` \quad (4.2)$$

where x_i^{k+1} is the updated position of particle *i.*

3. Evaluate Fitness:
    - Evaluate the fitness of each particle based on its position and objective function.
4. Update Personal Best and Global Best:
    - Update the personal best position (P_{best}) for each particle if a better solution is found.
    - Update the global best position (G_{best}) if a particle finds a better solution than the current global best.
5. Repeat Steps 2-5:
    - Iterate through Steps 2 to 5 until a termination condition is met (e.g., maximum number of iterations or desired fitness level achieved).

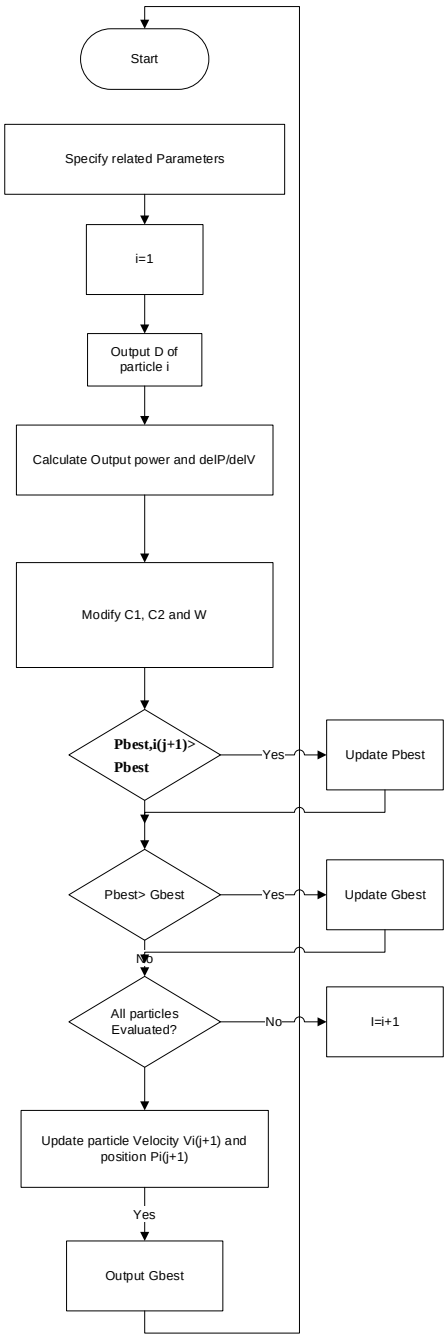

Fig 4.1. *Flowchart of Conventional PSO algorithm*

Flowchart of Conventional PSO is shown in fig 4.1. By repeatedly updating the velocities and positions of particles based on their own experiences and the best solutions found by the swarm, PSO optimizes the search process and aims to converge towards the optimal solution. Here is the flowchart for the conventional PSO algorithm. Reference [20] suggests an approach that recommends utilizing a particle swarm optimization (PSO) algorithm based on direct control for photovoltaic (PV) systems operating under mismatched conditions. In this method, three duty ratios

are employed as particles, and their initialization is based on the power-duty ratio characteristics that correspond to changes in irradiance. In [20] further enhance the tracking capability by introducing a deterministic PSO technique that eliminates the use of random numbers in the acceleration factor of the velocity equation. This approach is implemented on a buck-boost converter and compared to the Hill Climbing (HC) algorithm. Similarly, A modified PSO approach was suggested in reference [22] to track the global peak in scenarios where there are mismatches. This method builds upon the research conducted in reference [21]. This modification introduces the concept of a middle particle (d_{middle}) positioned between the minimum (d_{min}) and maximum (d_{max}) duty ratios for optimization during tracking. These advancements aim to improve the performance of PSO algorithms in maximizing power extraction from PV systems when faced with varying and mismatched operating conditions.

4.3 Adaptive Particle Swarm Optimization

The flowchart for adaptive PSO [8] is shown in Fig. 4.3. When the PSO convergence criteria is satisfied, the position of the particle represents maximum power taken from the system is stored as d_g. Next, a disturbance (Δd) is applied to duty cycle of the converter, and a new power is extracted from the PV system. Then, the fine adjustment is effectively carried out, in which the current power is more than the previous, the disturbance is kept in the similar direction. Above steps are repeated until the GMPP is tracked, or until the P and O convergence criteria is satisfied. The convergence criterion of is that the difference between the current and the previous power is less than the predefined limit as 1% using the relation mentioned in (4.3). In this application, the GMPP value generally changes with the environmental conditions.

$$\Delta P = \frac{Pm - P(m-1)}{Pm} < 1\% \tag{4.3}$$

The velocity of the algorithm is given by ().

$$\omega = \left\{\frac{\omega min - (\omega max - \omega min)(f - fmin)}{favg - fmin}\right\}, f \leq favg \tag{4.4}$$

$$\omega = \{\omega_{max}\},\ f \geq f_{avg} \tag{4.5}$$

In (4.4), f is particle's current fitness; f_{avg} is the average of whole set; f_{min} is least value & ω_{min} is 0.5, ω_{max} is 0.9.

The learning factor is introduced in the algorithm after same steps like PSO because each particle is different and changes dynamically according to its own fitness. As for the particle, the learning coefficient is given by (4.6) and (4.7).

$$c1(k) = c1(a1) + c1(b1)cos\frac{\pi k}{N_{max}} \quad (4.6)$$

$$c2(k) = c2(a2) - c2(b2)cos\frac{\pi k}{N_{max}} \quad (4.7)$$

Here, k is iteration number; N_{max} is max iteration number. The coefficient c1 represents the individual cognitive factor, indicating how much a particle learns from its own best state. On the other hand, the coefficient c2 represents the social cognitive factor, indicating how much a particle learns from the global best particle. The value of *c1* and *c2* in this paper is taken as *c1(b1)* = *c2(b2)* = 1.2, *c1(a1)* = 1.8, *c2(a2)* = 2. where *a1*, *a2*, *b1* and *b2* are the value of coefficients assigned to c1 and c2 taken from [8]. The conditions stated in (4.6) and (4.7) are used to identify reinitialization the APSO algorithm.

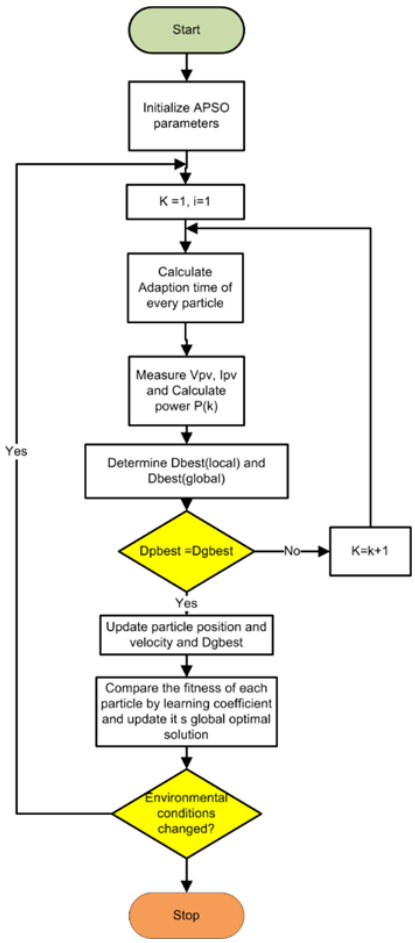

Fig. 4.3 *Flowchart for Adaptive Particle Swarm Optimization*

4.4 Hybrid P – O and Particle Swarm Optimization Technique

The flowchart of Hybrid PO-PSO is presented in Fig. 4.4 [13] Firstly, perturb and observe algorithm is initiated to locate the nearest local maxima. Further, the PSO method is employed to locate the global maxima. The time required for convergence can be greatly reduced as the search space is reduced. However, this technique cannot be used in the case of direct control of the converter duty cycle, as it uses the voltage of the photovoltaic system as a reference parameter, thus requiring a controller. Firstly, the complete search space is explored, and search is carried out in a reduced space until convergence. After a few calculation steps, it is possible to determine which particle is closest to the global maximum, then switches to the P & O algorithm [1]. Starting from the best particle, will perform an adjustment to find the GMPP. Every particle has a velocity and position in space. The particle positions are defined as the duty ratio of converter. The starting positions of the particles can be defined or assigned randomly in the search space. The particles that were initialized at equidistant positions in the interval [d_{min}, d_{max}], where d_{min} and d_{max} highlight the minimum and maximum duty ratio, respectively, of the energy converter. As for initial velocities of the particles, they are randomly assigned.

Next, the best individual and data related to global peak are updated. The power obtained is compared with the value of the vector $P_m(i)$ as indicated in Fig.7. This vector is initially zero and is used to store the best result for each particle. If current power is greater, $P_m(i)$ is updated and the duty cycle value is saved in the d_p vector. In continuation, the current power is compared with the best global power value (G_m). If the current power value exceeds the G_m, the G_m vector is updated and the duty cycle value is stored in the d_g variable. This process repeats until all particles have been evaluated. The next step, velocity and position of every particle in the swarm gets reconditioned. In conventional PSO algorithm, this update was given by previous step in which the inertial weight and the cognitive and social coefficients are constant. Whereas to accelerate convergence the velocity update is given by [13].

$$v_i^{(k+1)} = w^k v_i^{(k+1)} + \emptyset_1^k a_1(P_m - x_i^k) + \emptyset_2^k a_2(G_m - x_i^k) \quad (4.8)$$

The term $w^k v_i^{(k+1)}$ determine the convergence behavior of the PSO. Initially, it is a common practice to set the foremost weight w^k, is kept at high quantity for more convergence, moderately reduce it to obtain inertial weight,

$$w^k = w_{max} - \frac{k}{k_{max}}(\emptyset_{1,max} - \emptyset_{1,min}) \quad (4.9)$$

Where, w_{max} and w_{min} are the upper & lower threshold of weights respectively; k represents current iteration; k_{max} corresponds to the max allowable iterations; $\emptyset_1^k$ and $\emptyset_2^k$ that represent the cognitive and social actions are defined in (4.10) and (4.11), in that order.

$$\emptyset_1^k = \emptyset_{1,max} - \frac{k}{k_{max}}(\emptyset_{1,max} - \emptyset_{1,min}) \quad (4.10)$$

$$\emptyset_2^k = \emptyset_{2,min} + \frac{k}{k_{max}}(\emptyset_{2,max} - \emptyset_{2,min}) \quad (4.11)$$

Where, $\emptyset_{1,max}$, $\emptyset_{1,min}$ and $\emptyset_{2,max}$, $\emptyset_{2,min}$ are upper and lower thresholds of $\emptyset_1$ and $\emptyset_2$. Completion of first part of algorithm, two convergence criteria are determined. Firstly, the difference in positions of the particles is less than a limit, and second, if the algorithm reaches the maximum number of iterations. So, convergence limit must be chosen carefully, or the algorithm may go into later stage before reaching the global peak. Thus, in this research, the power limit was set to 10%, which is sufficient for the first stage to identify the proximities of the GMPP. As per empirical analysis, a limit of ten iterations is set to the first part of the algorithm. When one of the PSO convergence criteria is satisfied, the position of the particle that presents the highest power extracted from the system is stored in the d_g variable and transferred to the part of the hybrid algorithm that will perform a more refined adjustment. The second phase of the hybrid MPPT algorithm starts by applying the d_g work cycle in the converter. The value of power extracted from the photovoltaic system is tracked [13].

After applying a disturbance (Δd) to the duty ratio of the power converter, the new power is extracted from the PV system. Then, the fine adjustment is effectively carried out, in which the current power is more than the power obtained before to keep the disturbance same. Above steps

are repeated until the GMPP is tracked, or until the P and O convergence criteria is satisfied. The convergence criterion is the difference of current power and the previous one should be less than predefined limit (1%) using the relation mentioned in [13]. The GMPP value changes with environmental conditions and load conditions. Therefore, in order to enable the use of this PSO and P&O hybrid MPPT technique in dynamic situations, a power variation should be less than 10% or algorithm will reset the particle position and process repeats.

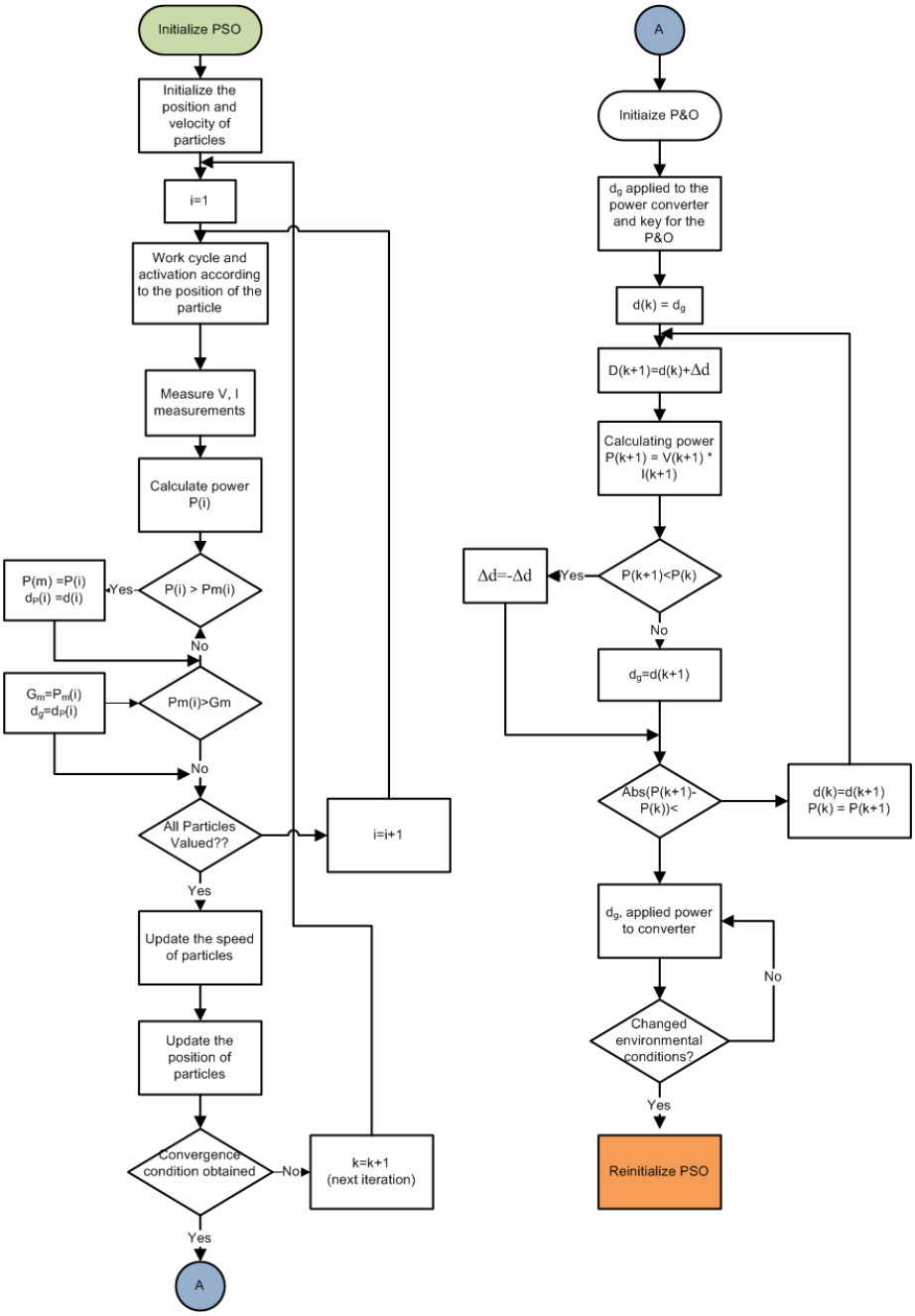

Fig 4.4. *Flowchart for PO -PSO based Hybrid PSO algorithm*

4.5 Conclusion

In this chapter, we have discussed the different Global peak tracking algorithm for tracking maximum power. According to complexity and implementation, Hybrid PO & PSO have more complexity and implementation as the algorithm has more logical approach for tracking different peaks at a particular point of time by setting the cognitive coefficient different than the conventional PSO. Whereas Adaptive PSO and Conventional PSO can be implemented with much more ease and also easy to understand. Thus, this Study has been concluded with the study of different tracking algorithm with a note that ease of implementation is kept as an essential point from the user's perspective.

CHAPTER 5

RESULTS AND DISCUSSION

5.1 Introduction

In this chapter, the results of the proposed Global tracking algorithms. This chapter is divided into two sections where first section includes the result of Conventional PSO based MPPT controller. The second section includes the result of Adaptive PSO based MPPT controller. The Third section includes the result of Hybrid PO - PSO based MPPT controller. Finally, the power results are then compared for calculating parameters tracking time, maximum Power output obtained and the Accuracy of the Algorithm. From the results we can draw the conclusion regarding which algorithm is suitable.

5.2 MATLAB Simulation Results of Conventional Particle Swarm Optimization based MPPT controller

In this section, the results of Conventional PSO based GMPPT is simulated in MATLAB-SIMULINK environment with the configuration shown below. Fig 5.1 represents the Boost converter with ESR with the MPPT controller.

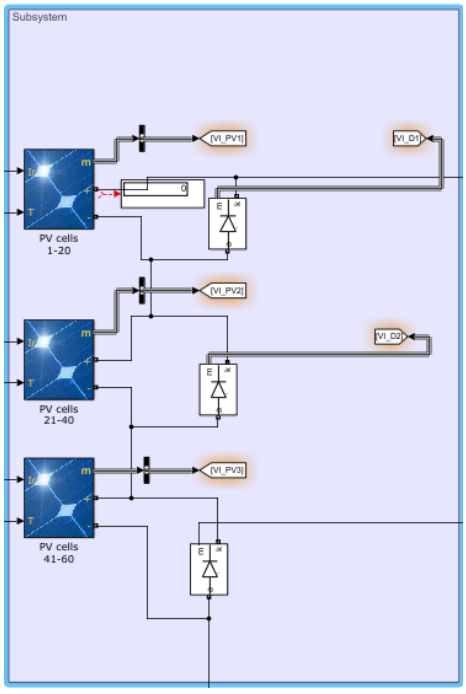

Fig. 5.1 *PV Module set for Single shading pattern*

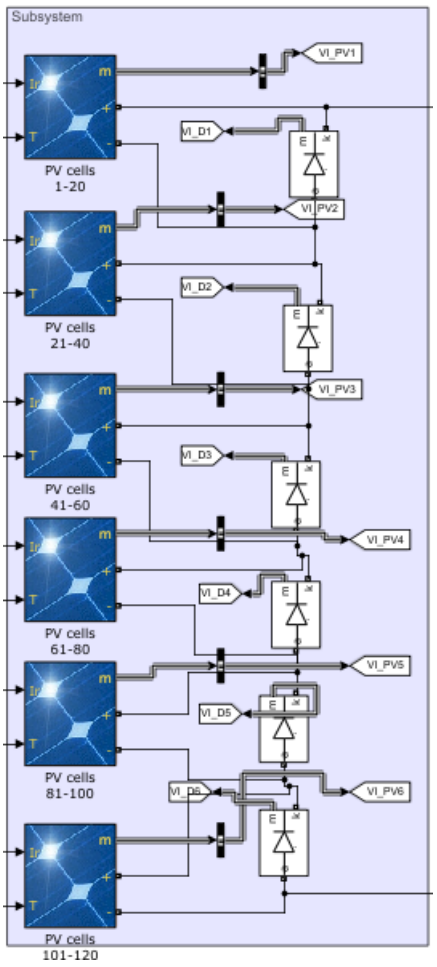

Fig. 5.2 *PV Module set for Multiple shading pattern*

5.2.1 Input & Output Power and Duty ratio

a) Irradiation [1000 1000 1000]

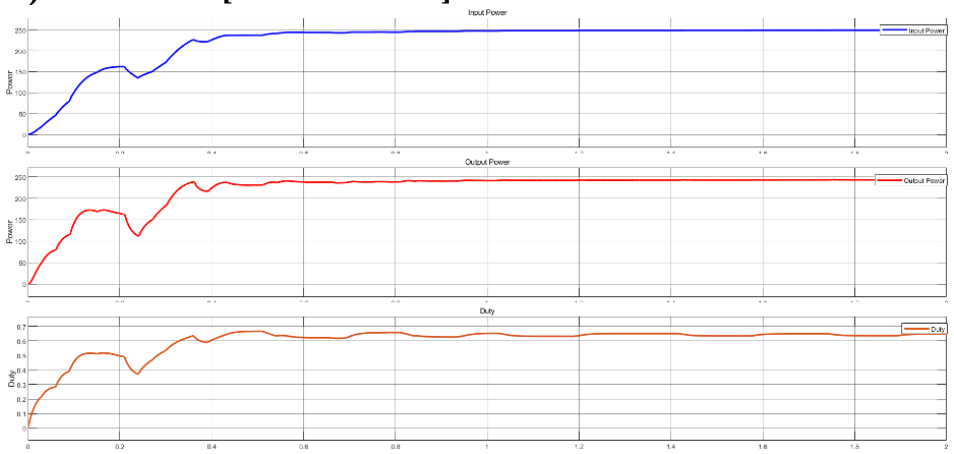

b) Irradiation [1000 800 600]

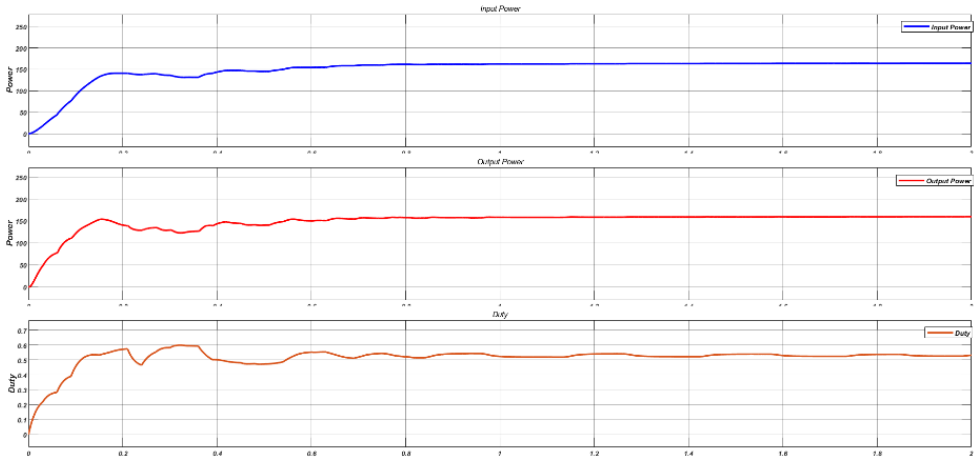

c) Irradiation [800 600 400]

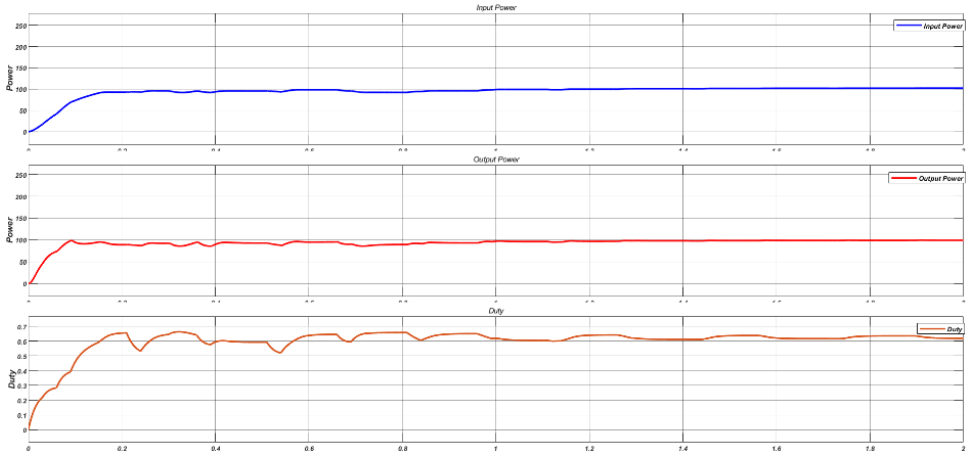

d) Irradiation [600 400 200]

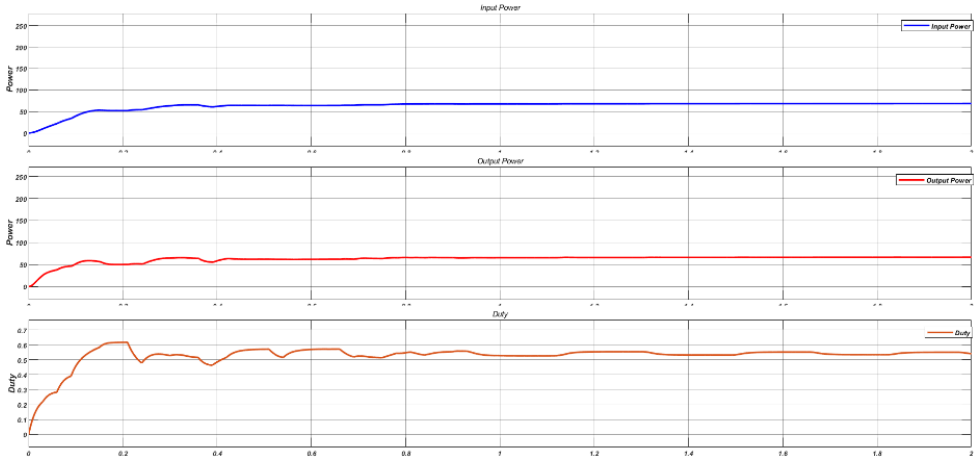

e) Irradiation for multi shading patterns [1000 1000 1000 1000 1000 1000]

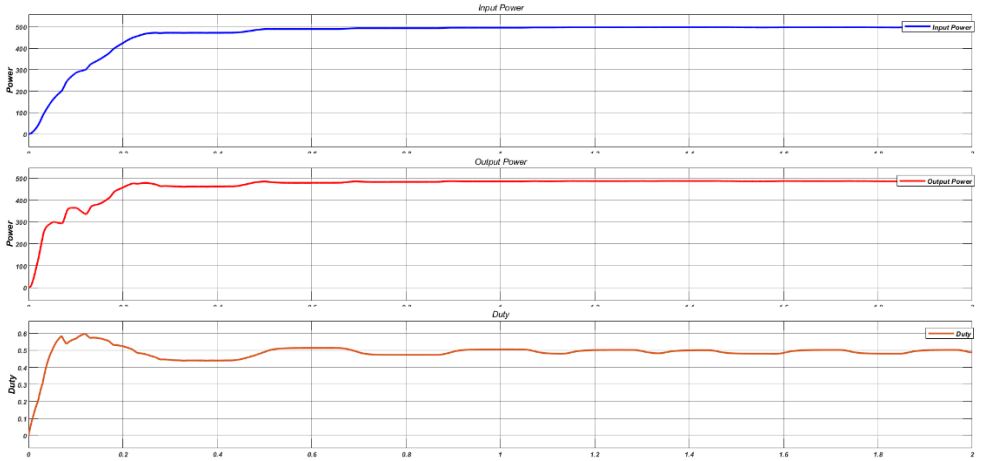

f) Irradiation for multi shading patterns [1000 1000 600 600 200 200]

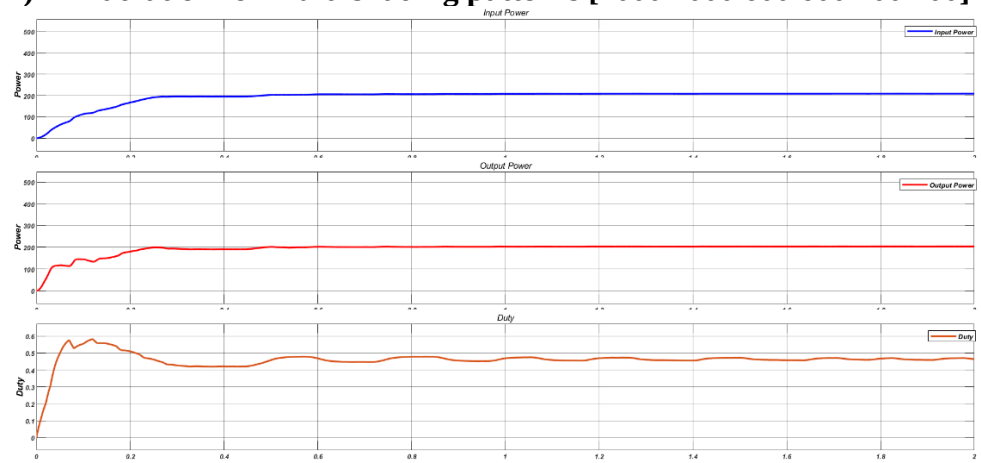

g) Irradiation for multi shading patterns [900 900 700 700 300 300]

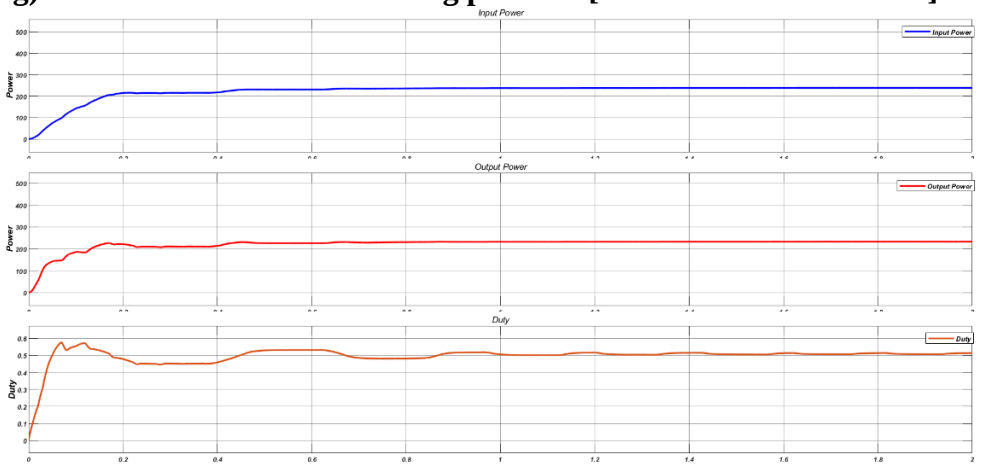

Fig 5.2.1 Waveforms of Power and Duty at a)[1000 1000 1000], b) [1000 800 600], c) [800 600 400], d) [600 400 200], e)[1000 1000 1000 1000 1000 1000], f))[1000 1000 600 600 200 200], g))[900 900 700 700 300 300]

5.2.2 Input and Output Voltage

a) Irradiation [1000 1000 1000]

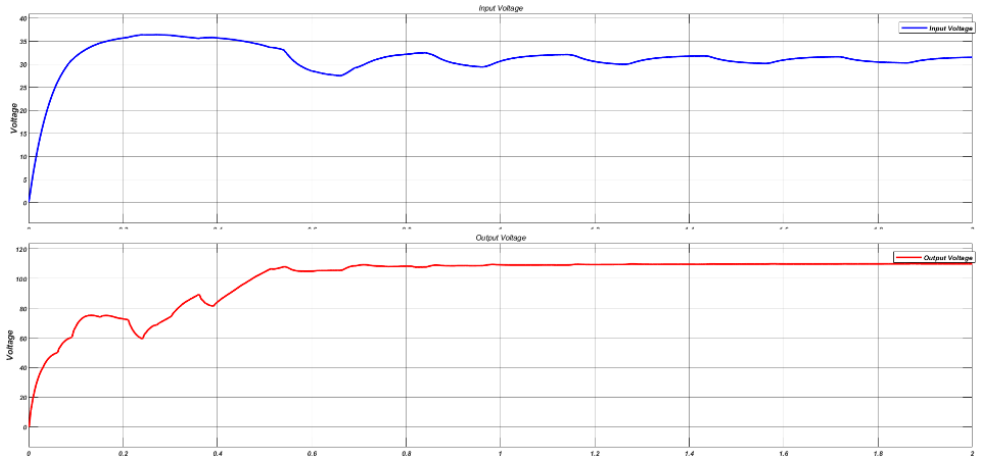

b) Irradiation [1000 800 600]

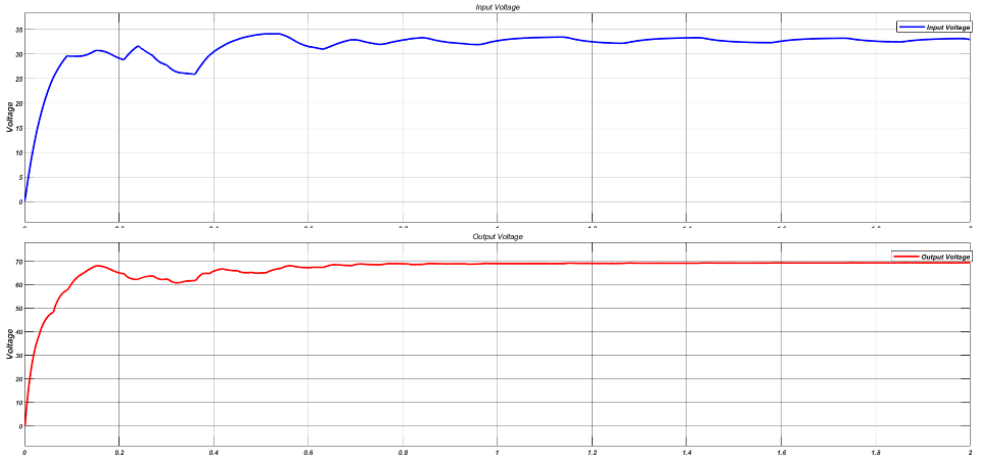

c) Irradiation [800 600 400]

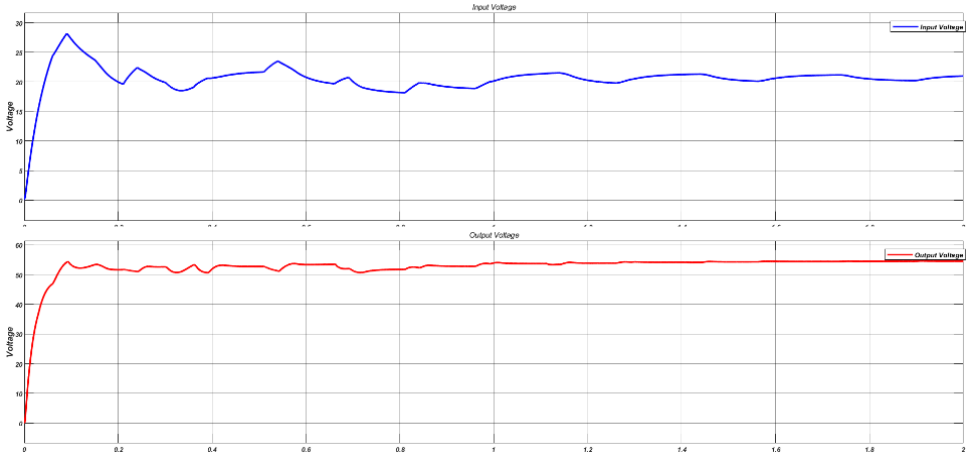

d) Irradiation [600 400 200]

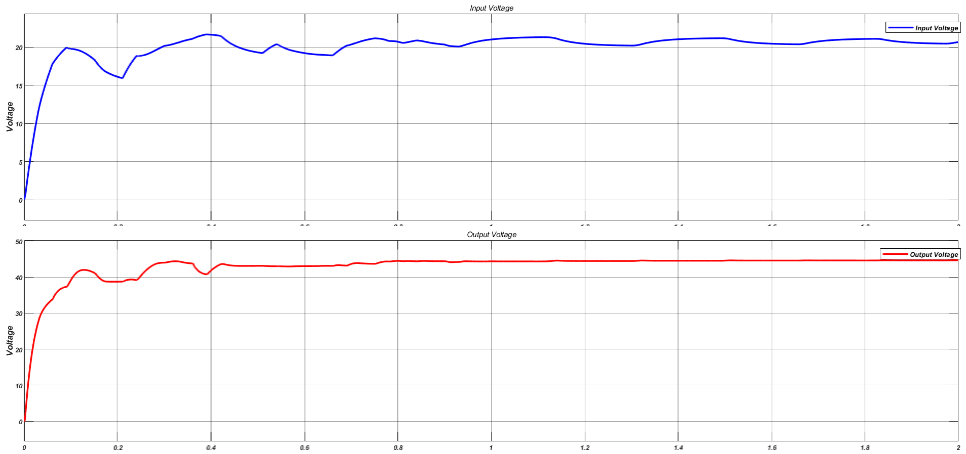

e) Irradiation for multi shading patterns [1000 1000 1000 1000 1000 1000]

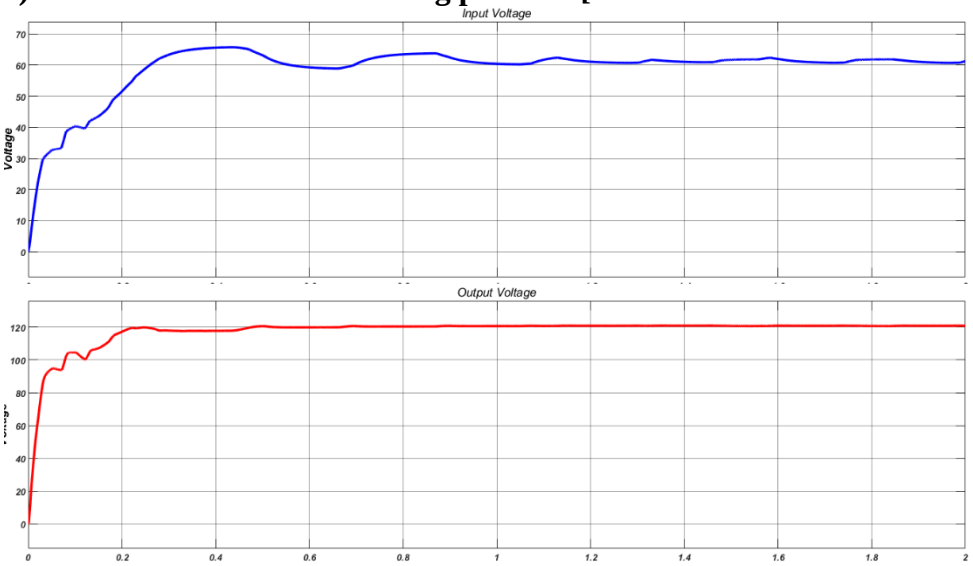

f) Irradiation for multi shading patterns [1000 1000 600 600 200 200]

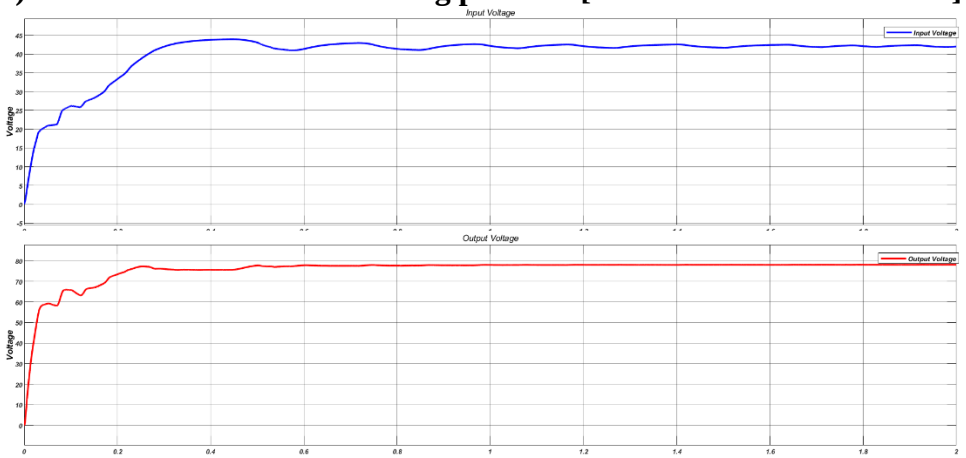

g) Irradiation for multi shading patterns [900 900 700 700 300 300]

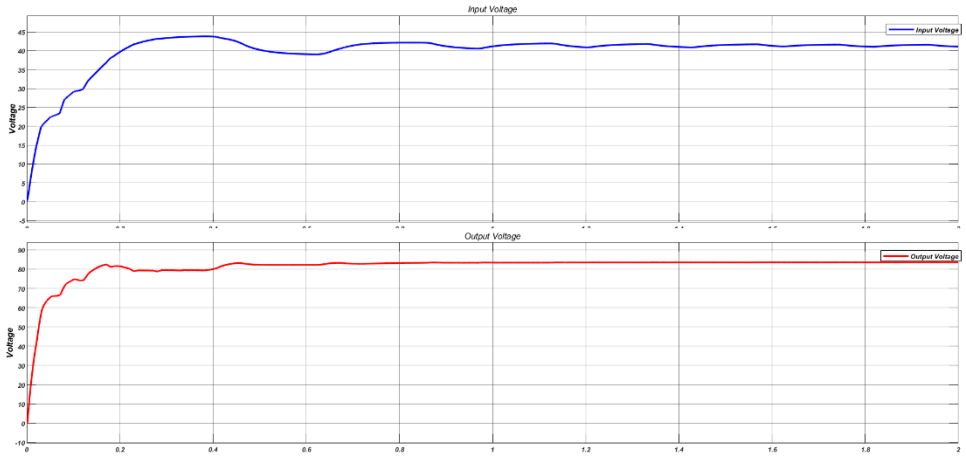

Fig 5.2.2 *Waveforms of Voltage at a) [1000 1000 1000], b) [1000 800 600], c) [800 600 400], d) [600 400 200], e)[1000 1000 1000 1000 1000 1000], f))[1000 1000 600 600 200 200], g))[900 900 700 700 300 300]*

5.3 MATLAB simulation Results of Adaptive Particle Swarm Optimization based MPPT controller

In In this section, the results of Adaptive PSO based GMPPT is simulated in MATLAB-SIMULINK environment with the configuration shown below.

5.3.1 Input & Output Power and Duty ratio

a) Irradiation [1000 1000 1000]

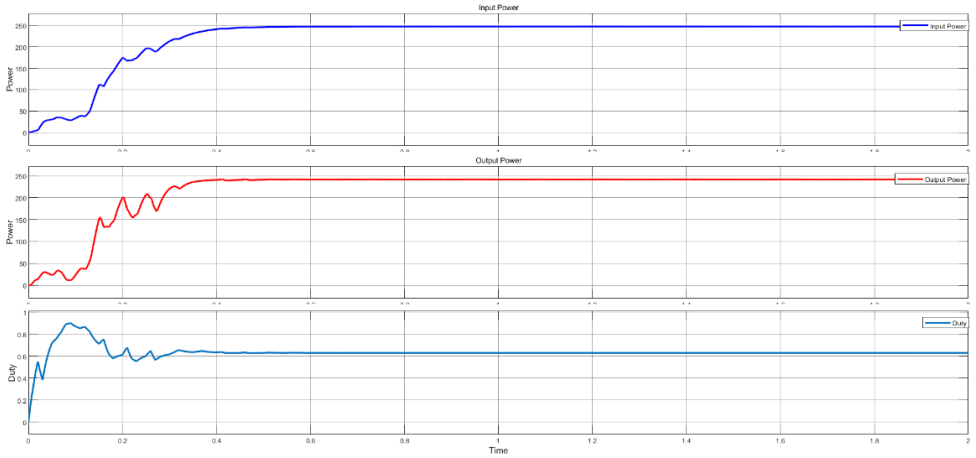

b) Irradiation [1000 800 600]

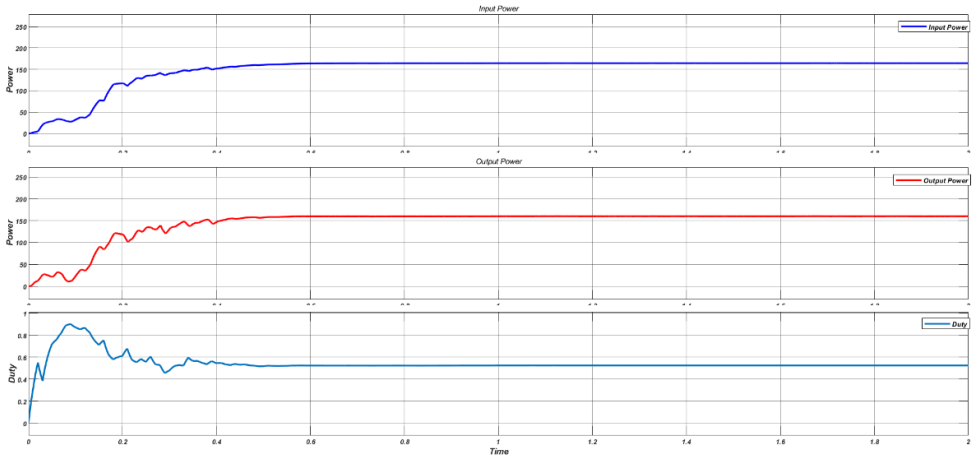

c) Irradiation [800 600 400]

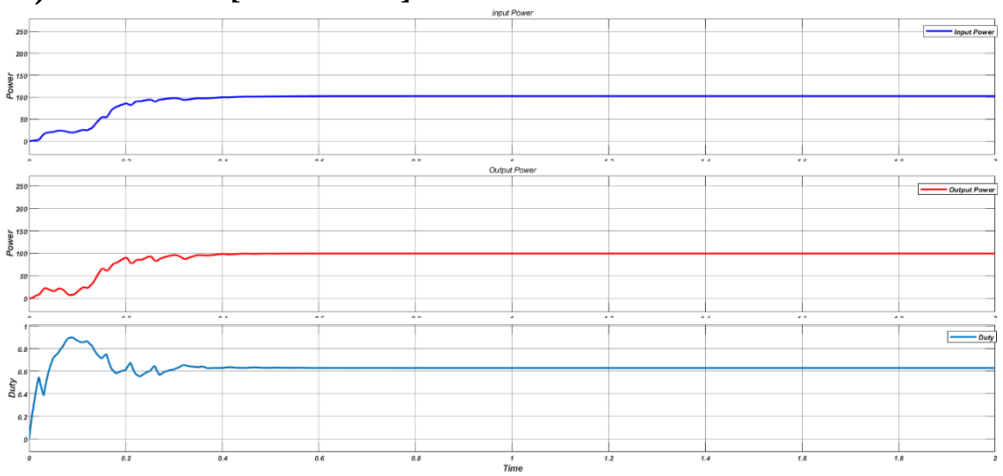

d) Irradiation [600 400 200]

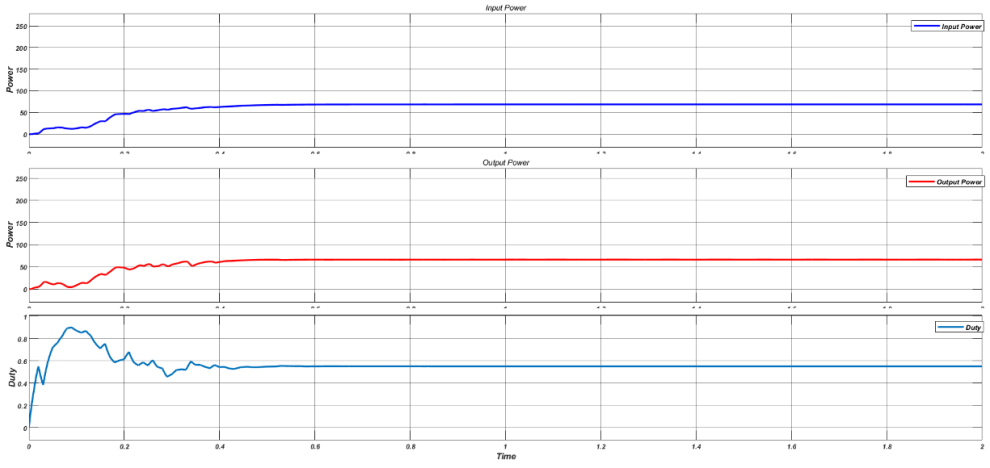

e) Irradiation for multi shading patterns [1000 1000 1000 1000 1000 1000]

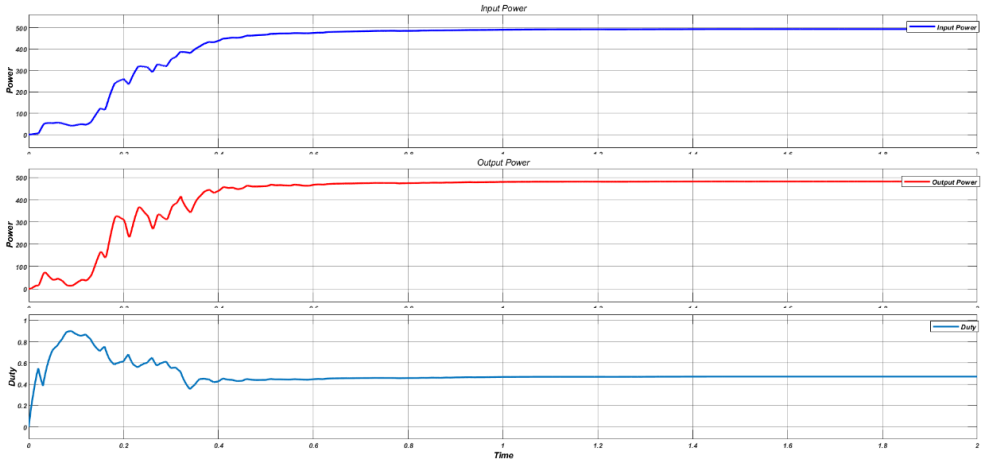

f) Irradiation for multi shading patterns [1000 1000 600 600 200 200]

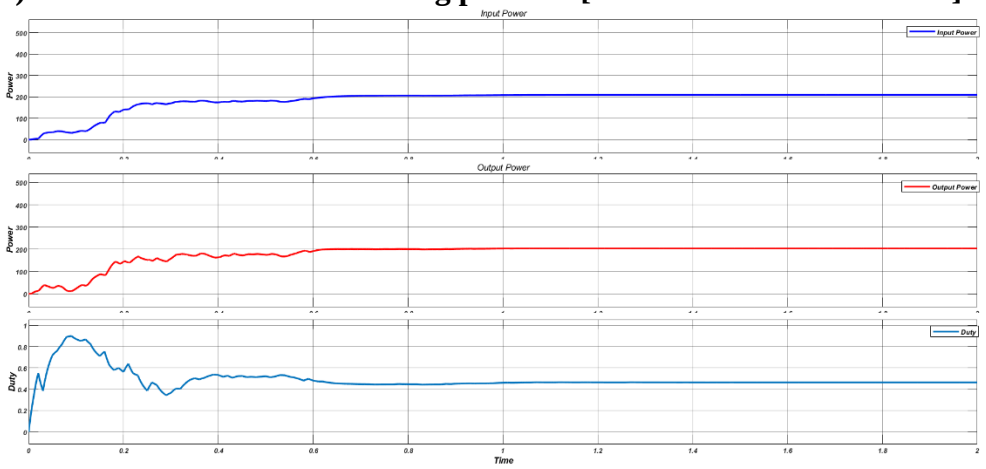

g) Irradiation for multi shading patterns [900 900 700 700 300 300]

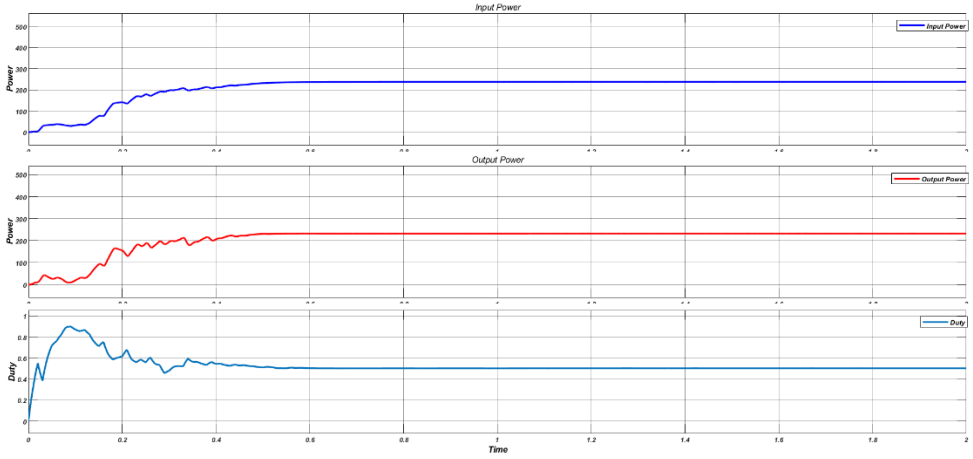

Fig 5.3.1 *Waveforms of Power and Duty Ratio at a)[1000 1000 1000], b) [1000 800 600], c) [800 600 400], d) [600 400 200], e)[1000 1000 1000 1000 1000 1000], f))[1000 1000 600 600 200 200], g))[900 900 700 700 300 300]*

5.3.2 Input and Output Voltage

a) Irradiation [1000 1000 1000]

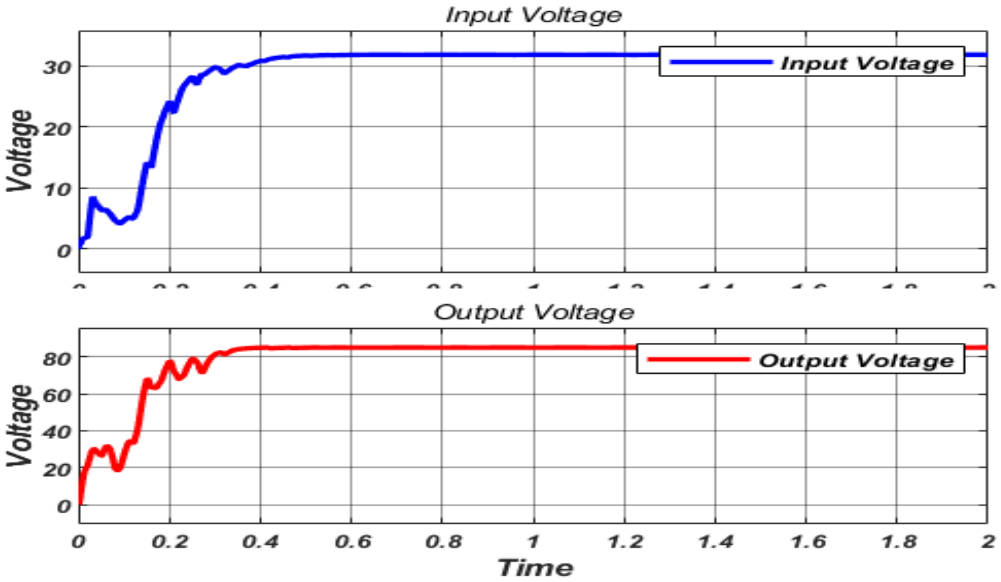

b) Irradiation [1000 800 600]

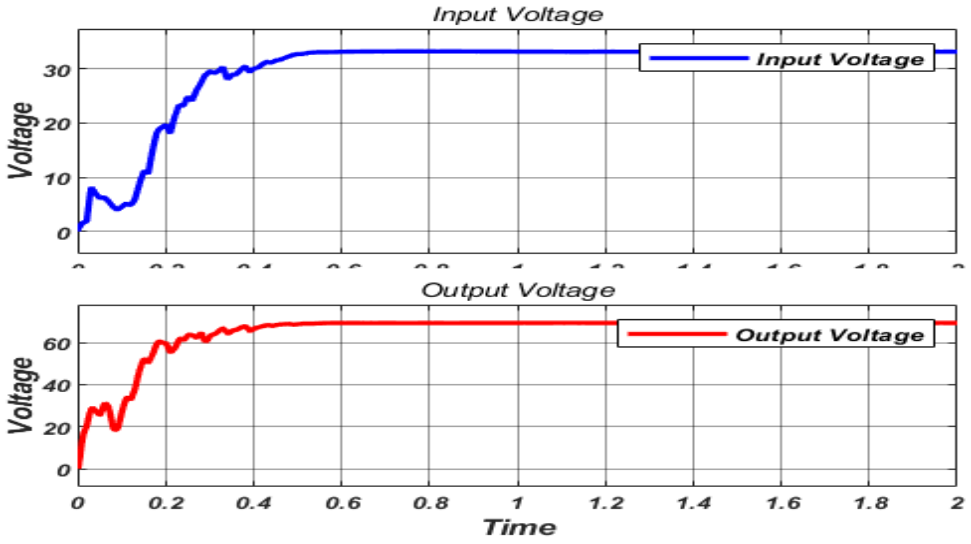

c) Irradiation [800 600 400]

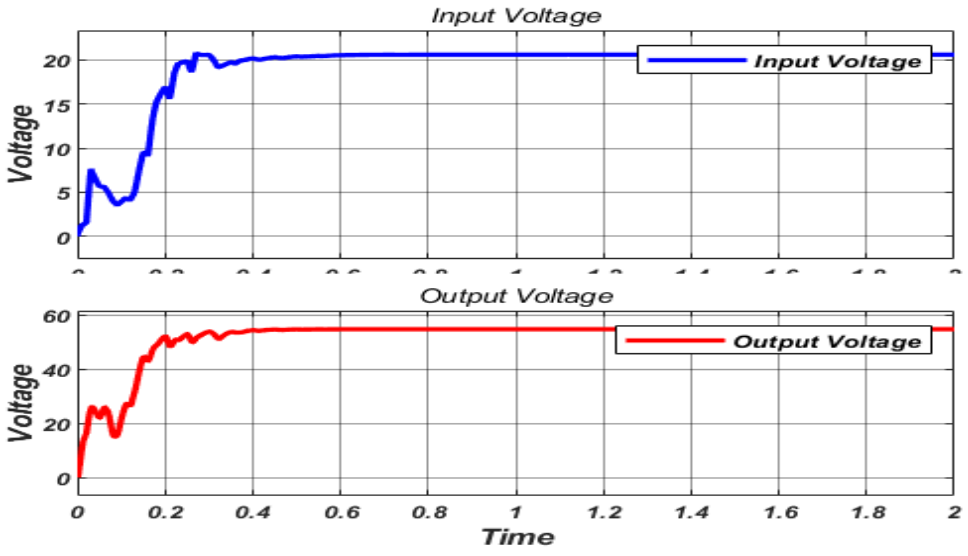

d) Irradiation [600 400 200]

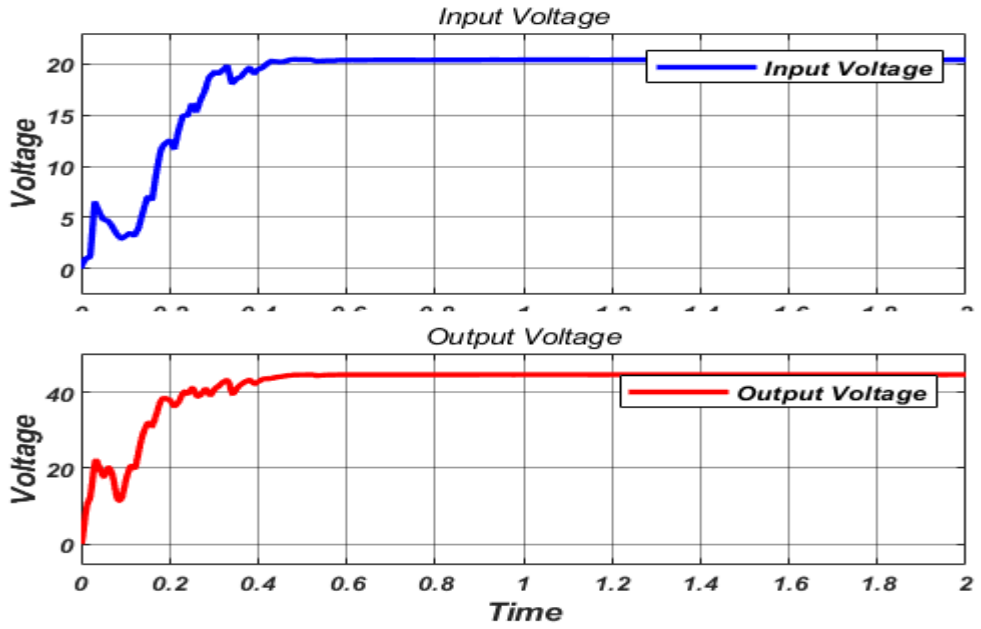

e) Irradiation for multi shading patterns [1000 1000 1000 1000 1000 1000]

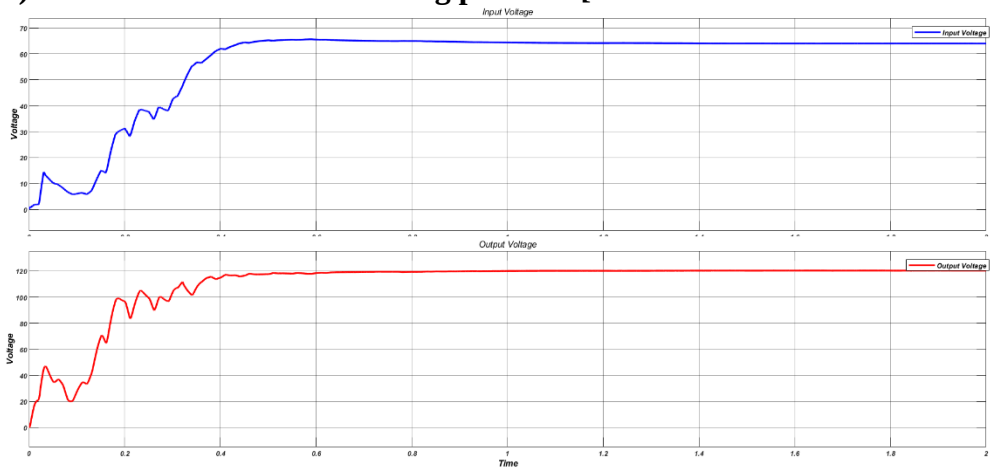

f) Irradiation for multi shading patterns [1000 1000 600 600 200 200]

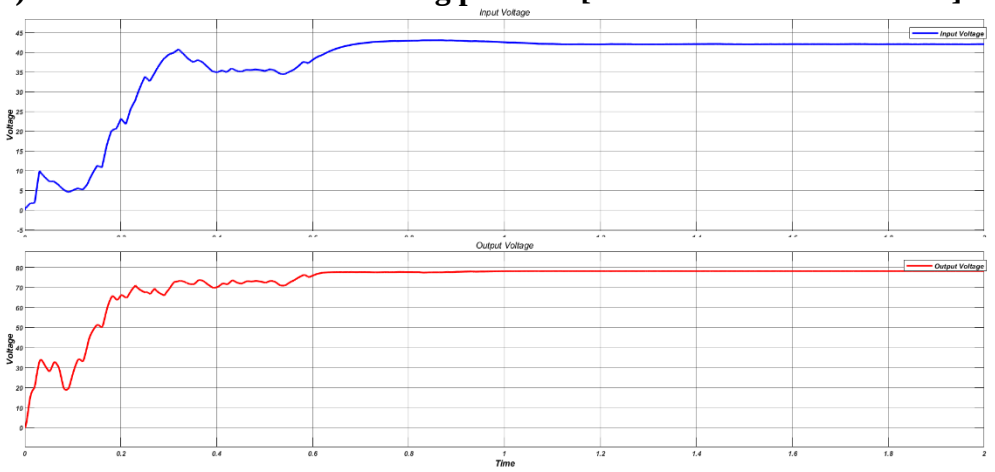

g) Irradiation for multi shading patterns [900 900 700 700 300 300]

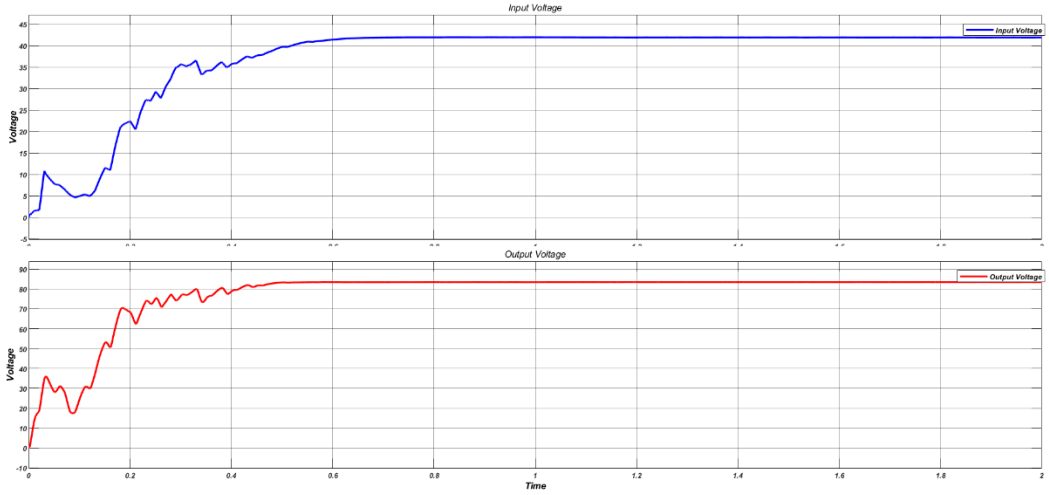

Fig 5.3.2 *Waveforms of Voltage at a)[1000 1000 1000], b) [1000 800 600], c) [800 600 400], d) [600 400 200], e)[1000 1000 1000 1000 1000 1000], f))[1000 1000 600 600 200 200], g))[900 900 700 700 300 300]*

5.4 MATLAB Simulation Results of Hybrid PO - Particle Swarm Optimization based MPPT controller

In In this section, the results of Hybrid PO - PSO based GMPPT is simulated in MATLAB-SIMULINK environment with the configuration shown below.

5.4.1 Input & Output Power and Duty Ratio

a) Irradiation [1000 1000 1000]

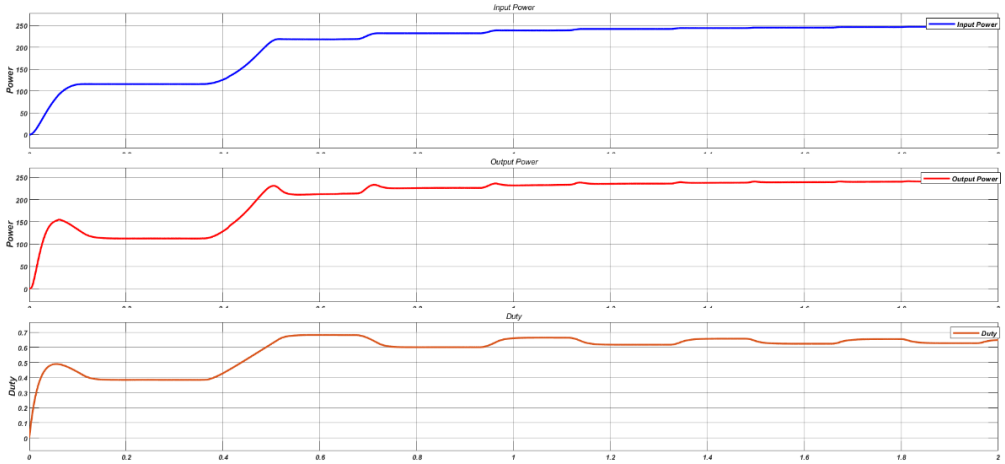

b) Irradiation [1000 800 600]

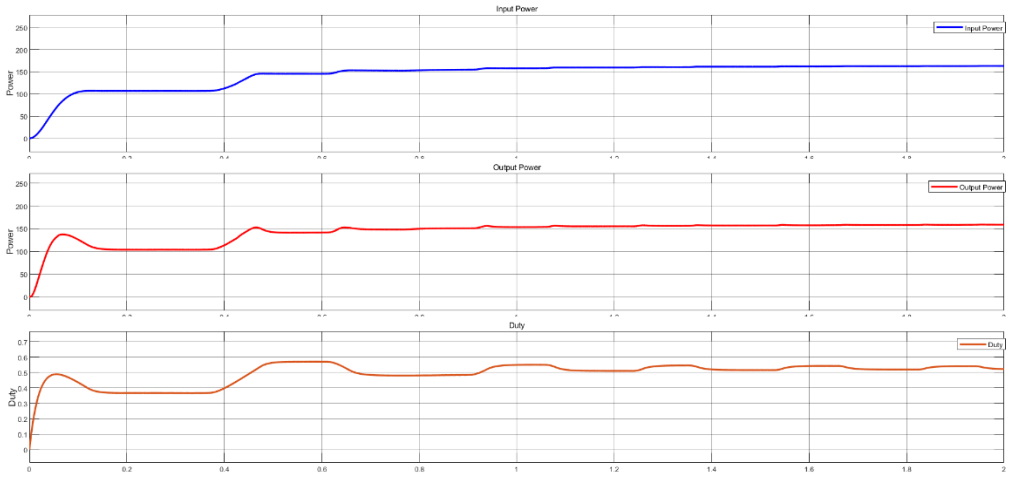

c) Irradiation [800 600 400]

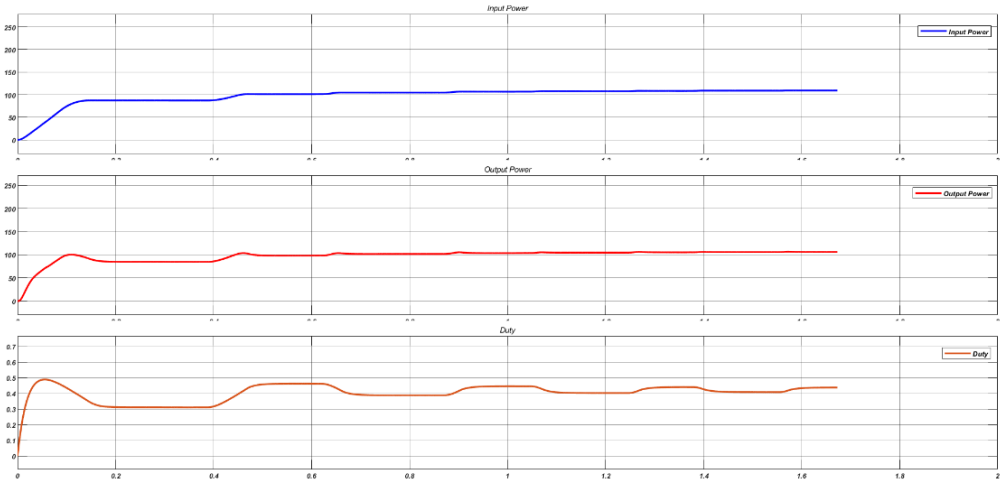

d) Irradiation [600 400 200]

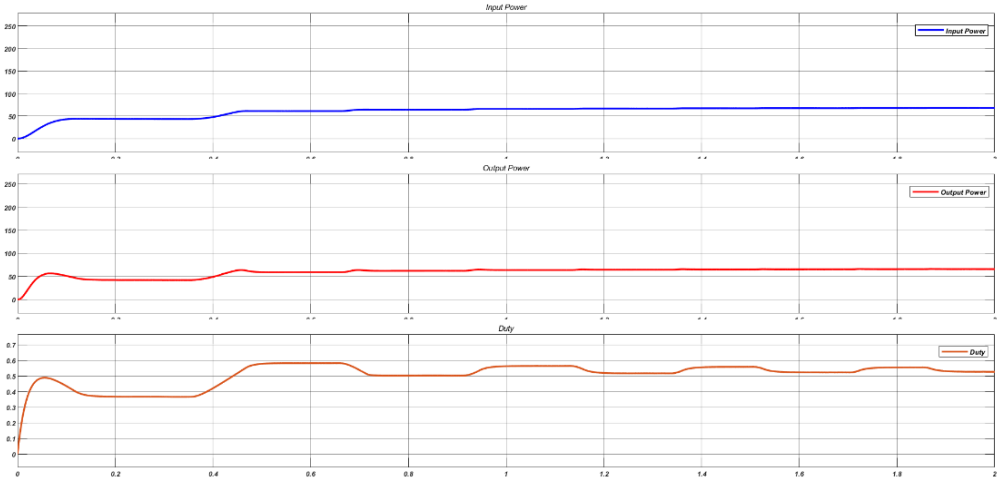

e) Irradiation for multi shading patterns [1000 1000 1000 1000 1000 1000]

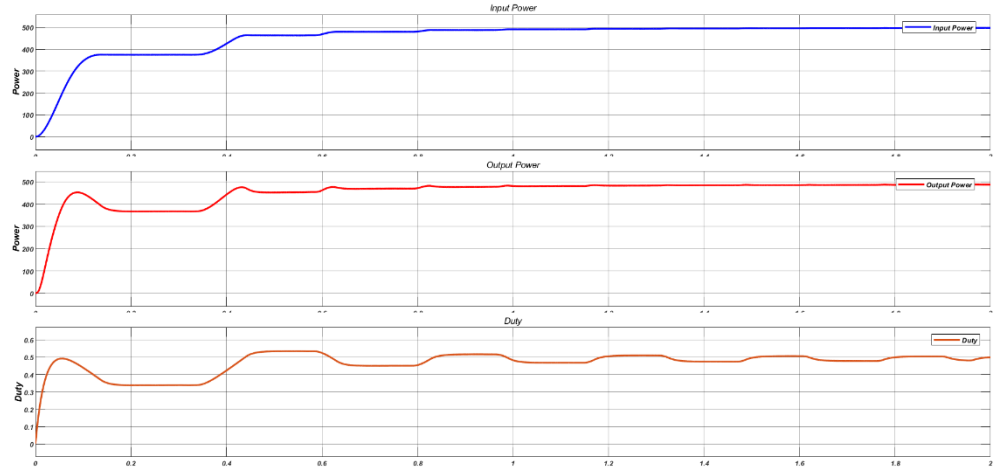

f) Irradiation for multi shading patterns [1000 1000 600 600 200 200]

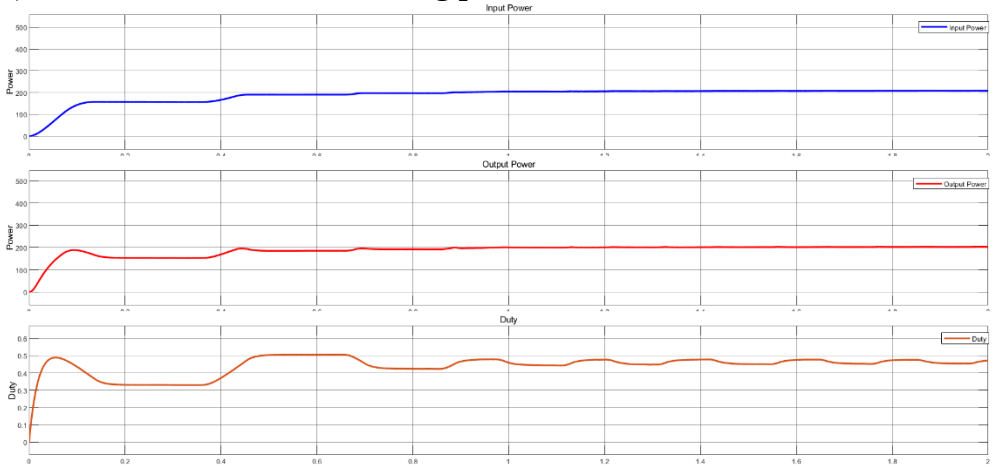

g) Irradiation for multi shading patterns [1000 1000 1000 1000 1000 1000] for modified Hybrid PO PSO

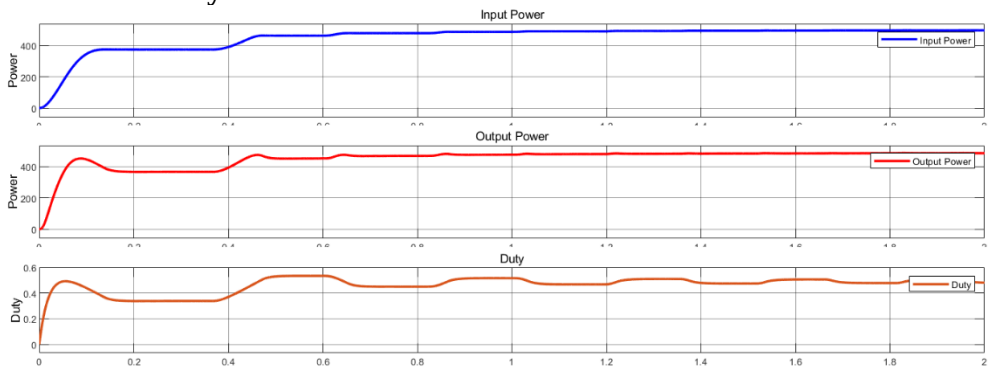

h) Irradiation for multi shading patterns [1000 1000 600 600 200 200] for modified Hybrid PO PSO

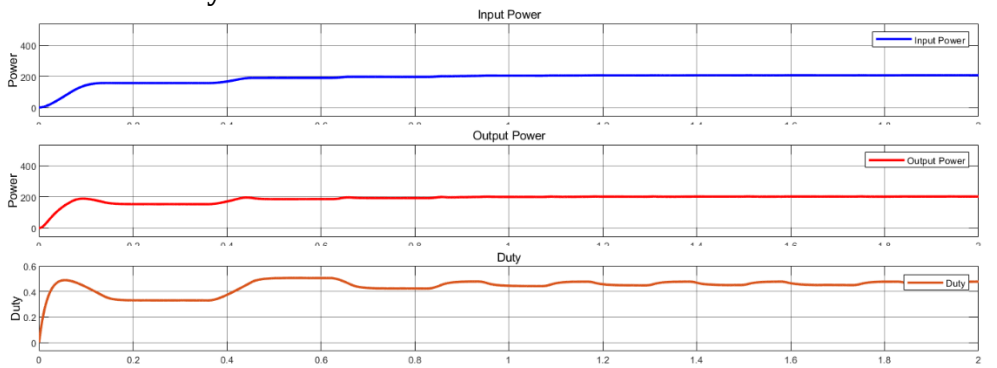

i) Irradiation for multi shading patterns [900 900 700 700 300 300] for modified Hybrid PO PSO

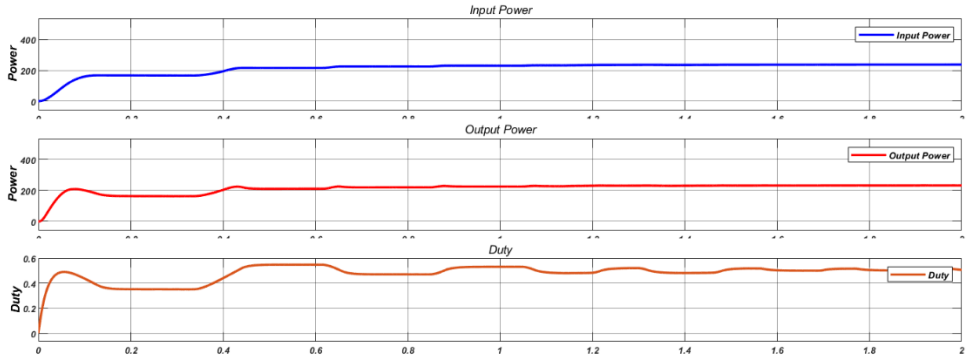

j) Irradiation for multi shading patterns [900 900 700 700 300 300]

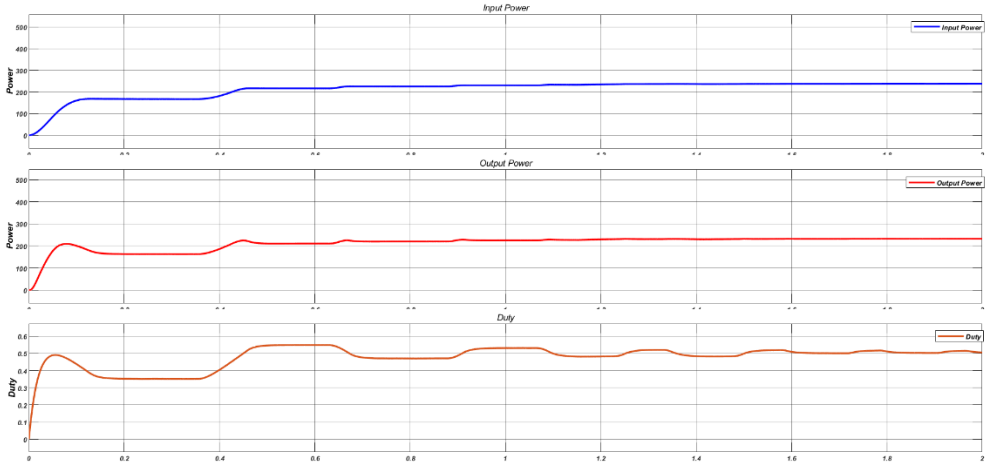

Fig 5.4.1 *Waveforms of Power and Duty Ratio at a)[1000 1000 1000], b) [1000 800 600], c) [800 600 400], d) [600 400 200], e)[1000 1000 1000 1000 1000 1000], f))[1000 1000 600 600 200 200], g))[900 900 700 700 300 300], i) [1000 1000 1000 1000 1000 1000] for Hybrid PO PSO j)[1000 1000 600 600 200 200] for hybrid PO PSO h) [900 900 700 700 300 300] for hybrid PO PSO*

5.4.2 Input & Output Voltage

a) Irradiation [1000 1000 1000]

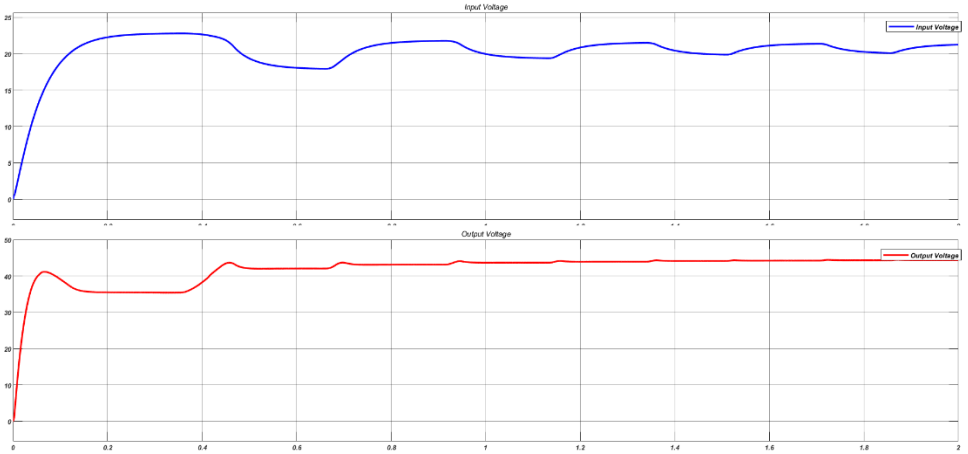

b) Irradiation [1000 800 600]

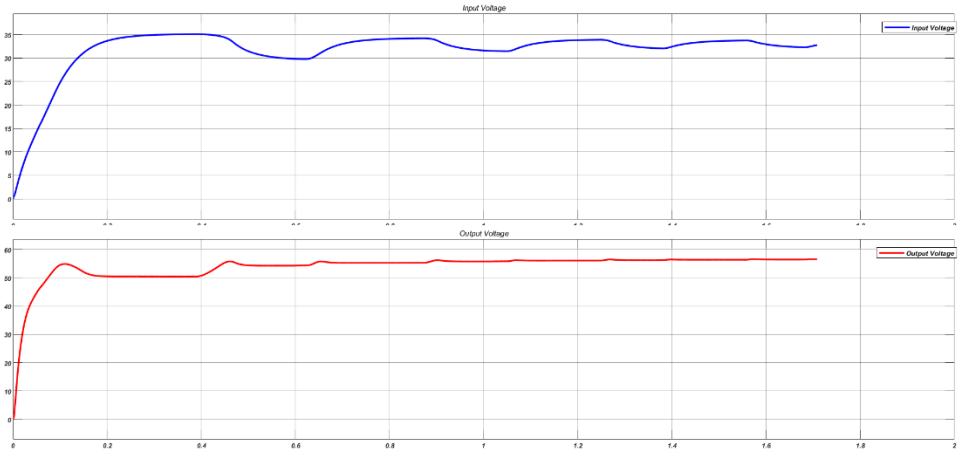

c) Irradiation [800 600 400]

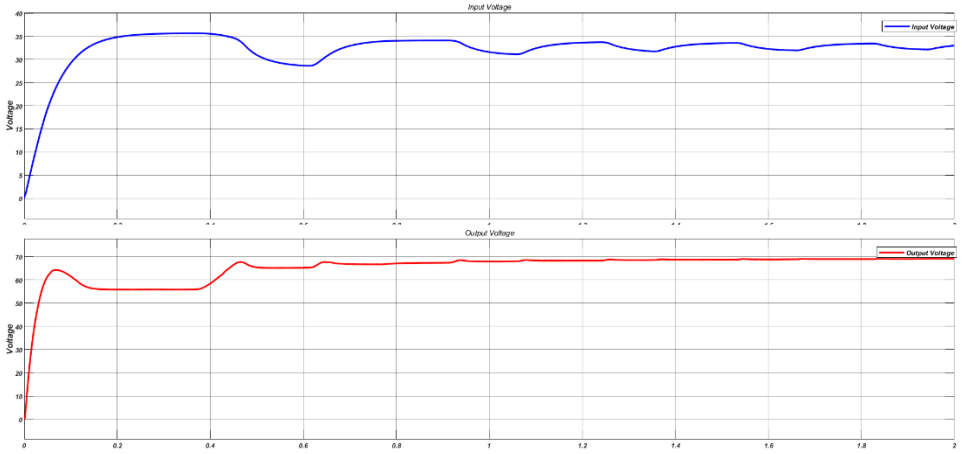

d) Irradiation [600 400 200]

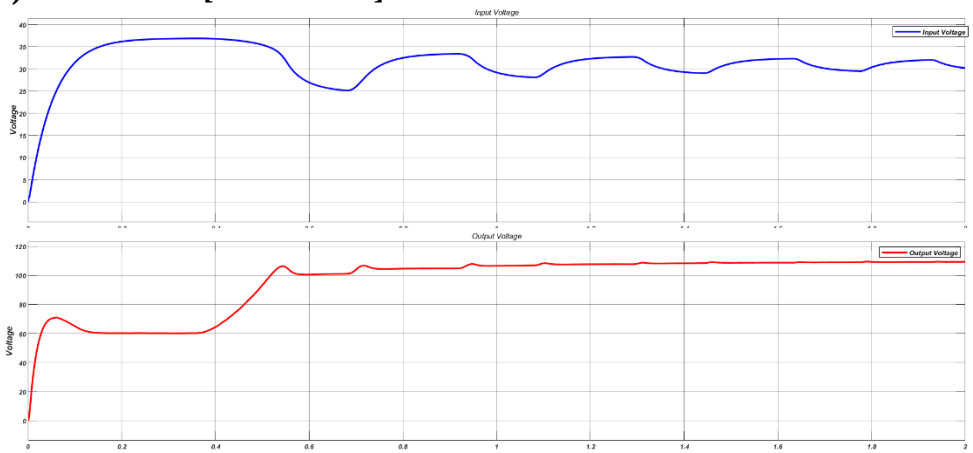

e) Irradiation for multi shading patterns [1000 1000 1000 1000 1000 1000]

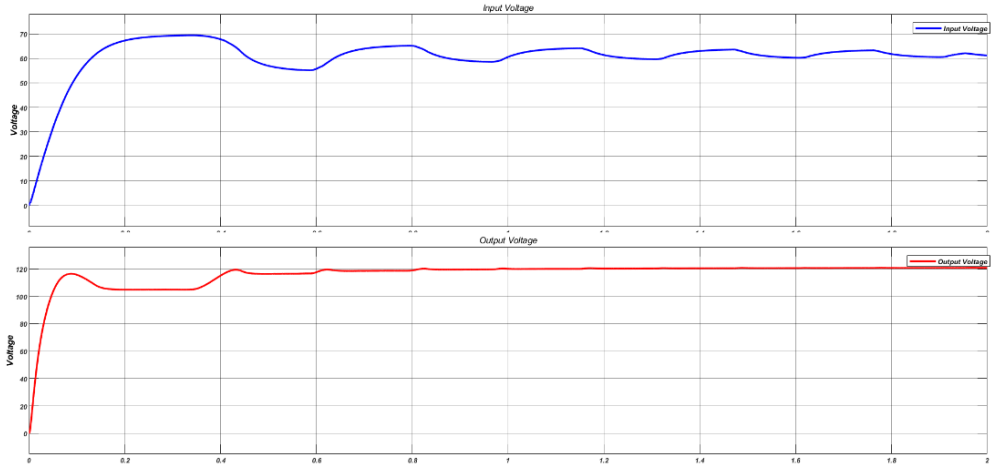

f) Irradiation for multi shading patterns [1000 1000 600 600 200 200]

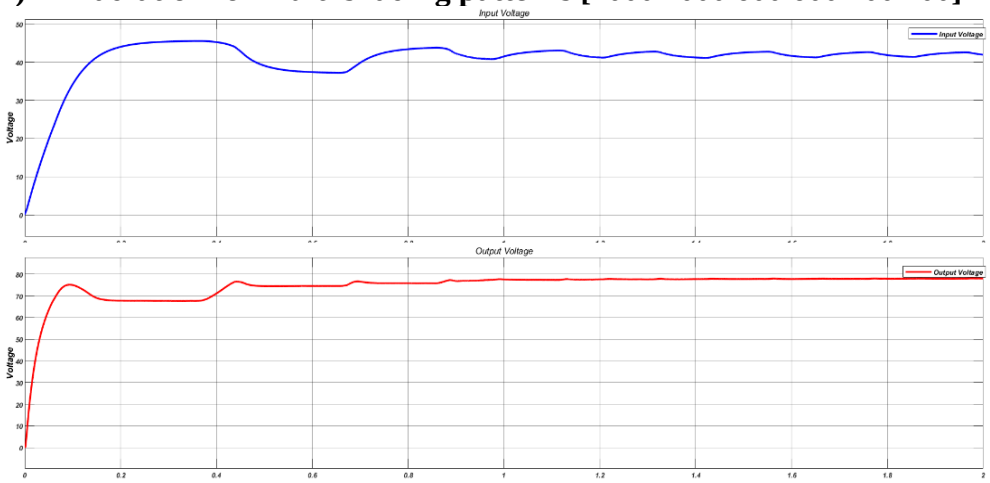

g) Irradiation for multi shading patterns [900 900 700 700 300 300]

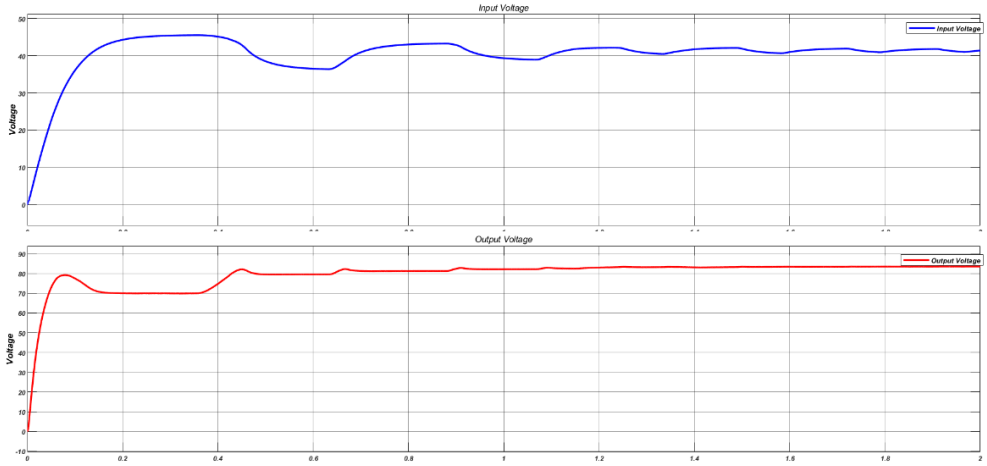

h) Irradiation for multi shading patterns [1000 1000 1000 1000 1000 1000] for modified Hybrid PO PSO

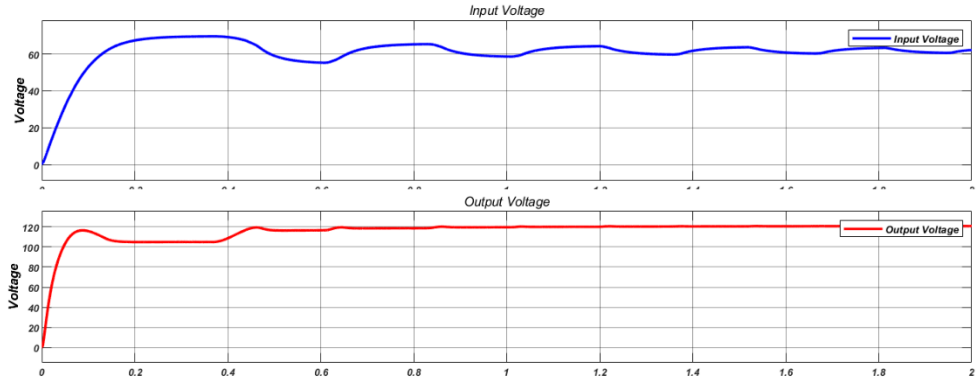

i)Irradiation for multi shading patterns [1000 1000 600 600 200 200] for modified Hybrid PO PSO

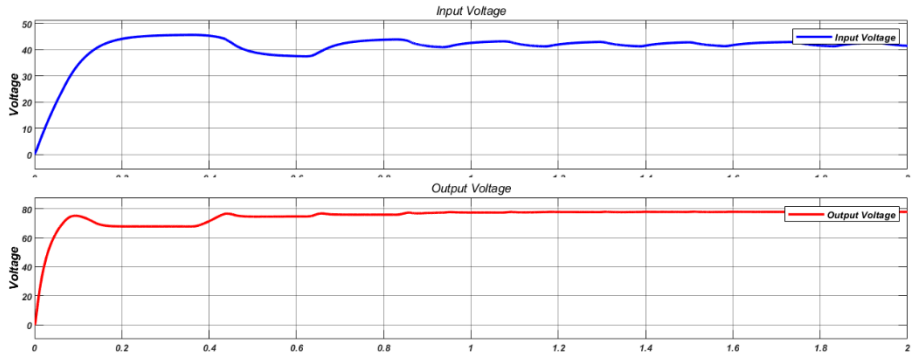

j) Irradiation for multi shading patterns [900 900 700 700 300 300] for modified Hybrid PO PSO

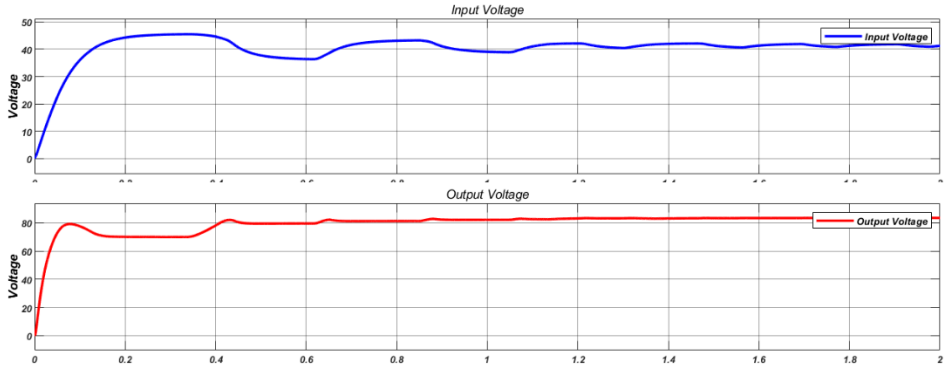

Fig 5.4.2 *Waveforms of Voltage at a)[1000 1000 1000], b) [1000 800 600], c) [800 600 400], d) [600 400 200], e)[1000 1000 1000 1000 1000 1000], f))[1000 1000 600 600 200 200], g))[900 900 700 700 300 300], i) [1000 1000 1000 1000 1000 1000] for Hybrid PO PSO j)[1000 1000 600 600 200 200] for hybrid PO PSO h) [900 900 700 700 300 300] for hybrid PO PSO*

5.5 Comparison Analysis of all Algorithms with Conclusion

Three PV Modules which are defined in Table I is considered for evaluation in this work. All three module with uniform irradiance at STC condition can generate the maximum power of 250 W. The effectiveness of all the algorithms is evaluated in terms of accuracy as per (5.1) [8].

$$Accuracy = \frac{P_{GMPP}}{P_{Steady\ state}} X100 \qquad (5.1)$$

a) Power plots for irradiance [1000 1000 1000]

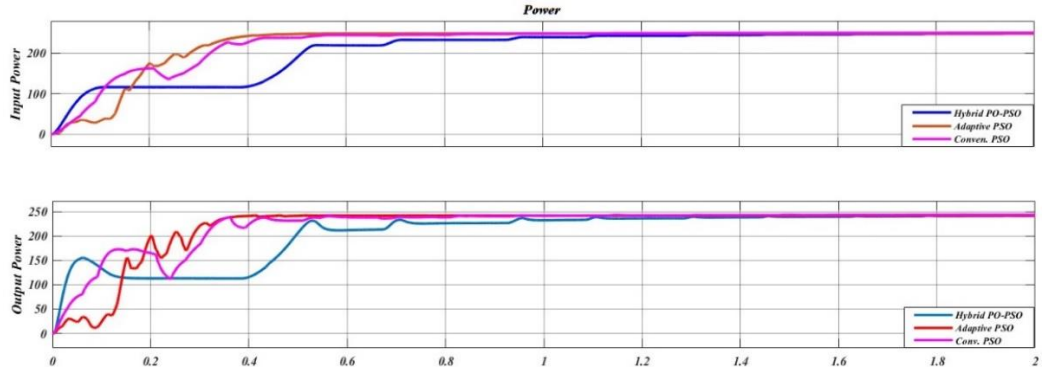

b) Power plots for irradiance [1000 800 600]

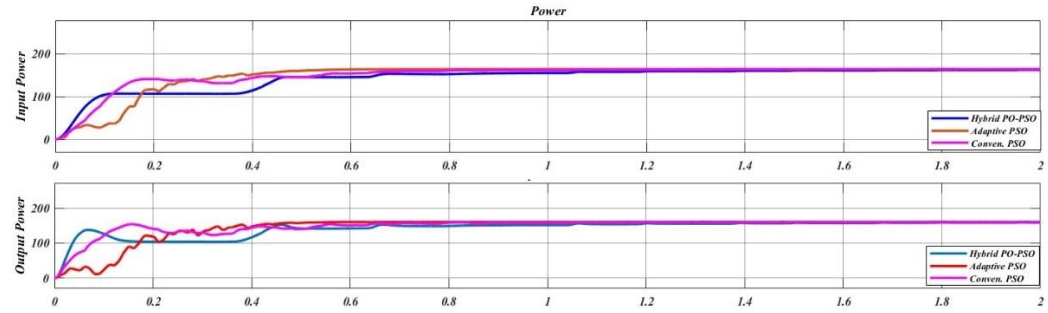

c) Power plots for irradiance [800 600 400]

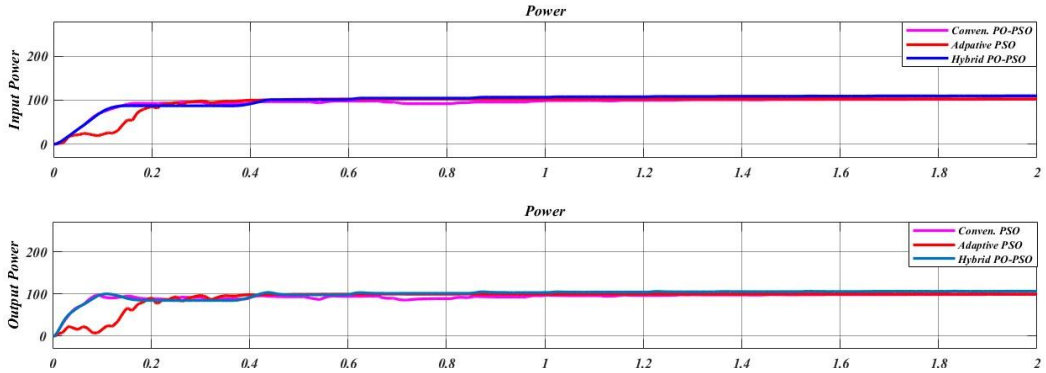

d) Power plots for irradiance [600 400 200]

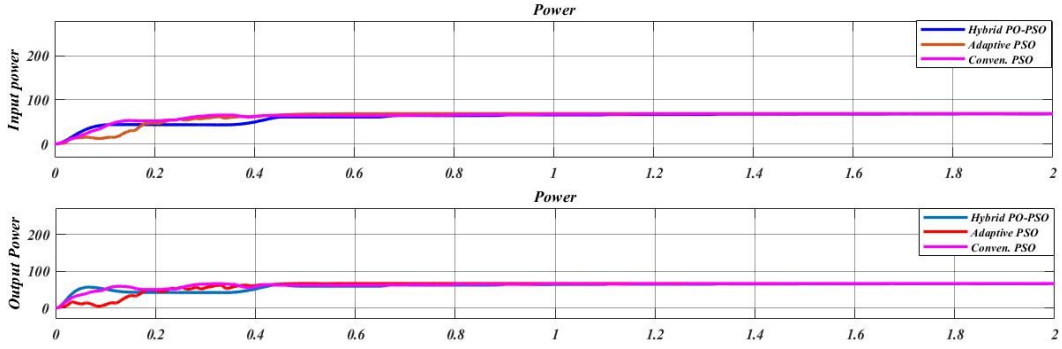

Fig 5.5 *Power Comparison results for Irradiance(a)[1000 1000 1000], (b) [1000 800 600], (c) [800 600 400] (d) [600 400 200]*

e) Power plots for irradiance [1000 1000 1000 1000 1000 1000]

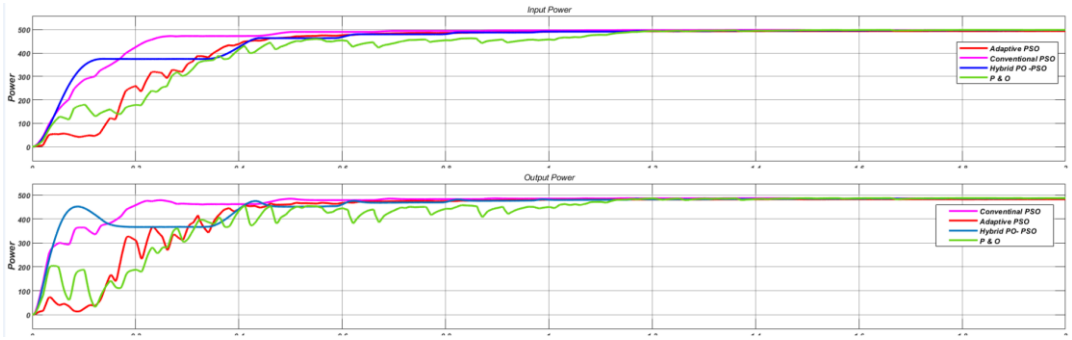

f) Power plots for irradiance [1000 1000 600 600 200 200]

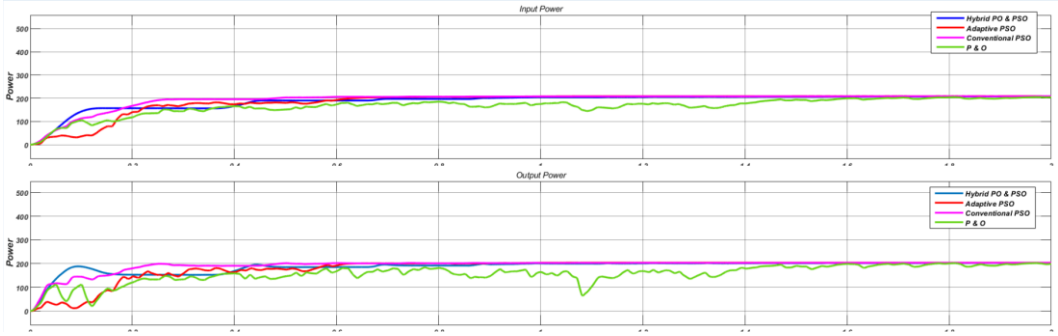

g) Power plots for irradiance [900 900 700 700 300 300]

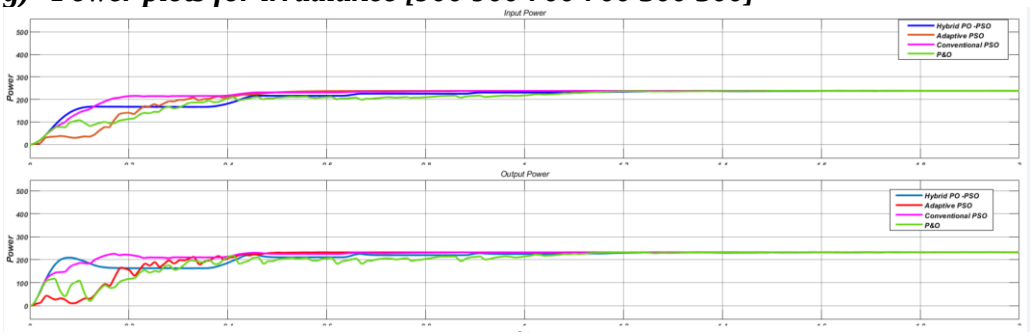

Fig 5.5 *Power Comparison results for Irradiance e)[1000 1000 1000 1000 1000 1000], f))[1000 1000 600 600 200 200], g))[900 900 700 700 300 300]*

TABLE V: COMPARATIVE ANALYSIS FOR DIFFERENT TRACKING ALGORITHMS USED IN SIMULATION

Algorithm	***Irradiation Set***	***Duty ratio***	***$P_{steady\ state}$ (W)***	***P_{GMPP}(W)***	***Accuracy (%)***	***Transient Time (T_s)***
Conventional. PSO	[1000 1000 1000]	0.6273	249.93	248.18	99.29%	0.83s
	[1000 800 600]	0.530	166.49	164.423	98.75%	0.67s
	[800 600 400]	0.415	110.01	108.28	98.84%	0.77s
	[600 400 200]	0.525	69.70	67.61	97.00%	0.65s
Adaptive PSO	[1000 1000 1000]	0.641	249.93	247.65	99.03%	0.57s
	[1000 800 600]	0.542	166.49	165.29	99.27%	0.63s
	[800 600 400]	0.625	110.01	107.22	97.74%	0.55s
	[600 400 200]	0.550	69.70	68.75	98.63%	0.67s
Hybrid PO-PSO	[1000 1000 1000]	0.652	249.93	249.20	99.70%	0.95s
	[1000 800 600]	0.549	166.49	166.20	99.82%	0.84s
	[800 600 400]	0.441	110.01	109.85	99.85%	0.43s
	[600 400 200]	0.587	69.70	69.34	99.48%	0.73s

In our second model based on a string of cells containing 6 PV cells, The model is run for the simulation time of 2 sec. From the analysis, it depicts that at steady state, the expected maximum power comes out to be 249.93W, Conventional PSO has an accuracy of 99.29 %, Adaptive PSO has accuracy of 99.03%, and Hybrid PO-PSO has an accuracy of about 99.70. In second case, dataset is taken as [1000 800 600] is shown in Fig.5.5 (b). The expected maximum power is 166.49 W, whereas from the simulation results, the conventional PSO has an accuracy of 98.75 %, adaptive PSO has accuracy of 99.27%, and hybrid PO-PSO has an accuracy of about 99.82%. From third case, the irradiance dataset taken is [800 600 400] as shown in Fig. 5.5 (c). The expected maximum power comes out to be 110.01W, whereas from our simulation results, we obtain that the conventional PSO has an accuracy of 98.84 %, adaptive PSO has accuracy of 97.74%, and hybrid PO-PSO has an accuracy of about 99.85%. The irradiance dataset in final stage taken is [600 400 200] as shown in Fig. 5.5 (d). The expected maximum power comes out to be 69.70W, we obtain that the Conventional PSO has an accuracy of 97.00%, adaptive PSO has accuracy of 98.63%, and Hybrid PO-PSO has an accuracy of about 99.48%. Thus, Hybrid techniques bags the credit for average maximum accuracy among all three. However, if we observe the tracking time of simulation results of all algorithms, then Hybrid PO-PSO is slower in some cases than adaptive PSO. In a conclusion a tradeoff can be made between peak tracking time and performance accuracy for selecting a desired algorithm.

Algorithm	*Irradiation Set*	*Duty ratio*	$P_{steady\ state}$ *(W)*	P_{GMPP}*(W)*	*Accuracy (%)*	*Transient Time* (T_s)
Conventional. PSO	[1000 1000 1000 1000 1000 1000]	0.478	500	493.2	98.64	0.670
	[1000 1000 600] [600 200 200]	0.493	209	202.8	97.03	0.664
	[900 900 700] [700 300 300]	0.527	239	233.4	97.65	0.689
Adaptive PSO	[1000 1000 1000 1000 1000 1000]	0.438	500	496.7	99.34	0.724
	[1000 1000 600] [600 200 200]	0.441	209	207.8	99.42	0.691
	[900 900 700] [700 300 300]	0.453	239	235.1	98.36	0.731
Hybrid PO-PSO	1000 1000 1000 1000 1000 1000]	0.523	500	497.8	99.56	0.78
	[1000 1000 600] [600 200 200]	0.481	209	208.3	99.66	0.724
	[900 900 700] [700 300 300]	0.504	239	236.7	99.03	0.725
Modified Hybrid PO-PSO	[1000 1000 1000 1000 1000 1000]	0.484	500	498	99.60	0.80
	[1000 1000 600] [600 200 200]	0.476	209	208.4	99.69	0.88
	[900 900 700] [700 300 300]	0.508	239	238.2	99.66	1.09
P&O	1000 1000 1000 1000 1000 1000]	0.468	500	491.2	98.24	1.21
	[1000 1000 600] [600 200 200]	0.532	209	200	95.69	0.97
	[900 900 700] [700 300 300]	0.489	239	230.4	96.40	1.09

TABLE VI: COMPARATIVE ANALYSIS FOR DIFFERENT TRACKING ALGORITHMS USED IN SIMULATION FOR MULTIPLE SHADING

In the second run taking multiple shading patterns, The model is run for the simulation time of 2 sec. From the analysis, it depicts that at steady state, the expected maximum power comes out to be 500W for 6 modules attached in series in a string with irradiance in first case as [1000 1000 1000 1000 1000 1000], the accuracy of Conventional PSO has an accuracy of 98.64 %, Adaptive PSO has accuracy of 99.34%, and Hybrid PO-PSO has an accuracy of about 99.56, Modified Hybrid PO-PSO has an accuracy of 99.60 and lastly P & O took the longest time to track with accuracy of 98.24%. In second case, dataset is taken as [1000 1000 600 600 200 200] is shown in

Fig.5.6 (b). The expected maximum power is 209 W, whereas from the simulation results, the conventional PSO has an accuracy of 97.03 %, adaptive PSO has accuracy of 99.46%, and hybrid PO-PSO has an accuracy of about 99.62%, Modified Hybrid PO-PSO has an accuracy of 99.69% and P & O again tracks the peak taking the maximum time with an accuracy of 95.69%. In final case, dataset is taken as [900 900 700 700 300 300] is shown in Fig.5.6 (c). The expected maximum power is 239 W, whereas from the simulation results, the conventional PSO has an accuracy of 97.65 %, adaptive PSO has accuracy of 98.36%, and hybrid PO-PSO has an accuracy of about 99.03%, Modified Hybrid PO-PSO has an accuracy of 99.66% and P & O again tracks the peak taking the maximum time with an accuracy of 96.40%.

From the Observations, we can conclude few points as follows:

1. ***Tracking Speed:*** Tracking speed depends upon the how quickly the algorithm achieves it steady state value. In the study, it was found that adaptive PSO algorithm was found faster than any other algorithm. However, Hybrid PO-PSO and Modified hybrid PO -PSO took more time in reaching settling space due to larger search space. Whereas, PO is not suited for this as it neither had faster response nor provides stability in response.
2. ***Coverage of Algorithm***: Coverage of algorithm refers to the search space the algorithm searches before reaching the output. In study based on the 300 iterations, Modified Hybrid PO-PSO engages a larger search space for duty cycle going from 0 to 0.8. Whereas, other algorithms like PSO are defined for a limited search space i.e. for duty cycle of 0.2 to 0.7.
3. ***Ease of use***: Ease of use is essential from the user point of view. In case of optimized algorithms, PSO has fewer variables to set as compared to other algorithms like Fuzzy logic etc. Therefore, PSO is preferred choice for the amateur. For more accuracy, Modified Hybrid PO -PSO sets different parameters for calculating cognitive coefficients, thus takes some time to settle to the steady state.
4. ***Power loss:*** The P&O algorithm takes more time and power before settling. As in figure 5.5(e), the ripple in power for P&O are higher. Thus, P&O is not an appropriate option as it doesn't always provide Global maxima for a given P – V characteristics.

In summary, our study enhances the knowledge of global maximum power point

tracking (GMPPT) techniques and offers valuable insights for optimizing solar PV systems, particularly in scenarios involving partial shading. On Comparing the algorithms, the disadvantage of the Hybrid PO-PSO is it has longer tracked time but gives us a greater accuracy as compared to other two with least error margin. However, the other two algorithm have less tracking time but with smaller accuracy as compared to Hybrid PO-PSO. For higher accuracy, we prefer Hybrid PO-PSO for maximum extracted PV power. For least tracking time, it depends solely on a user needs and design. For the Implementation perspective, Hybrid algorithm is quite difficult to design as the cognitive coefficients are expressed in terms which depend on the performance of the neighboring particle as compared to conventional PSO. These GMPPT techniques are studied under the application of partial shading with no fast-changing environment as they will require more power input for initializing the algorithm after every change in environment which is not favorable. Thus, this study concludes under non -uniform partial shading conditions whose analysis can further studied by done by taking different shading patterns for different modules.

CHAPTER 6

CONCLUSION AND FUTURE SCOPE

6.1 Conclusion

In conclusion, the investigations on global peak tracking algorithms for extracting maximum power in PV systems have yielded valuable insights and advancements in the field. The use of hybrid PSO-PO algorithms, adaptive PSO algorithms, and conventional PSO algorithms has shown promising results in improving the performance and efficiency of PV systems.

The hybrid PSO-PO algorithm synergistically integrates the advantages of particle swarm optimization (PSO) and pattern optimization (PO) techniques, resulting in enhanced convergence speed and precision. This approach enables effective tracking of the global peak, even in demanding scenarios characterized by factors like partial shading or fluctuating irradiance levels.

The adaptive PSO algorithms, on the other hand, incorporate adaptive mechanisms to dynamically adjust the algorithm parameters based on the system's behaviour. This adaptability enhances the algorithm's robustness and enables effective tracking of the MPP under different environmental conditions and system variations. Conventional PSO algorithms have also been extensively studied and utilized for global peak tracking in PV systems. These algorithms provide a reliable and efficient approach to optimize the power output and ensure maximum energy extraction from the PV array.

Overall, the investigations on these global peak tracking algorithms have highlighted their effectiveness in improving the performance of PV systems. However, further research is still needed to explore their full potential and address certain challenges, such as convergence speed, robustness in dynamic environments, and the need for accurate modelling and parameter tuning.

In conclusion, the hybrid PSO-PO algorithm, adaptive PSO algorithms, and conventional PSO algorithms offer valuable options for optimizing global peak tracking in PV systems. Their application can significantly to improve the energy harvesting efficiency and overall performance of photovoltaic (PV) systems, various strategies can be employed, contributing to the advancement of renewable energy technologies.

6.2 Future Scope

The Future work scope regarding Global Peak Tracking Algorithm can be listed as following:

1. Multi-Objective Optimization: Future research can focus on integrating multi-objective optimization techniques to simultaneously optimize power output, minimize losses, and reduce costs in global peak tracking algorithms.
2. Hybrid Converters: There is potential for improving global peak tracking algorithms by incorporating hybrid converters, such as combining boost and buck converters. These converters offer advantages like improved efficiency, reduced voltage stress, and increased flexibility, but their implementation requires careful control strategies and thorough analysis.
3. Distributed MPPT: The future of global peak tracking algorithms could involve the development of distributed MPPT, where individual MPPT units are used for each module or group of modules in a solar PV array. This approach enhances system reliability, mitigates the impact of partial shading, and allows for scalability. However, coordination and optimal operation of multiple MPPT units present challenges.
4. Advanced Control Techniques: Future research can explore advanced control techniques like model predictive control (MPC), fuzzy logic control, and Digital controlling algorithms to enhance the accuracy and efficiency of global peak tracking. These techniques are especially valuable in complex operating conditions and dynamic environments, but implementation requires robust algorithms, accurate models, and real-time computational capabilities.

In summary, future advancements in global peak tracking algorithms involve multi-objective optimization, hybrid converters, distributed MPPT, and advanced control techniques which can be implemented via various converter according to desired applications.

REFERENCES

[1] J M. A. Elgendy, B. Zahawi, and D. J. Atkinson, "Assessment of Perturb and Observe MPPT Algorithm Implementation Techniques for PV Pumping Applications," IEEE transactions on sustainable energy, vol. 3, no. 1, pp. 21–33, 2011.

[2] S. Motahhir, A. El Ghzizal, S. Sebti, and A. Derouich, "Modeling of photovoltaic system with modified incremental conductance algorithm for fast changes of irradiance," International Journal of Photoenergy, vol. 2018, 2018.

[3] S. M. Adam, H. Wen, J. Ma, K. Wang, and K. L. Man, "An Improved P&O MPPT Method Using Boost Converter for Photovoltaic applications," in International Conference on Recent Advancements in Computing in AI, Internet of Things (IoT) and Computer Engineering Technology (CICET), 2020, pp. 26–28.

[4] A. Mohapatra, B. Nayak, and K. Mohanty, "Current Based Novel Adaptive P&O MPPT Algorithm for Photovoltaic System Considering Sudden Change in The Irradiance," in 2014 IEEE International Conference on Power Electronics, Drives and Energy Systems (PEDES). IEEE, 2014, pp. 1–4.

[5] M. Nasiri, S. Chandra, M. Taherkhani, and S. J. McCormack, "Impact of Input Capacitors in Boost Converters on Stability and Maximum Power Point Tracking in PV Systems," in 2021 IEEE 48th Photovoltaic Specialists Conference (PVSC). IEEE, 2021, pp. 1004–1008.

[6] S. Silvestre, A. Boronat, and A. Chouder, "Study of Bypass Diodes Configuration on PV Modules," Applied Energy, vol. 86, no. 9, pp. 1632–1640, 2009.

[7] W. Hayder, E. Ogliari, A. Dolara, A. Abid, M. Ben Hamed, and L. Sbita, "Improved PSO: A Comparative Study in MPPT Algorithm for PV System Control Under Partial Shading Conditions," Energies, vol. 13, no. 8, p.2035, 2020.

[8] X. Chen, Y. Chai, and Y. Wang, "Application Of Adaptive Particle

Swarm Optimization in Multi-Peak MPPT of Photovoltaic Array," in 2020 IEEE 4th Information Technology, Networking, Electronic and Automation Control Conference (ITNEC), vol. 1. IEEE, 2020, pp. 165–169.

[9] D. W. Hart, Power Electronics, McGraw-Hill New York, 2011.

[10] M. Arjun, V. V. Ramana, R. Viswadev, and B. Venkatesaperumal, "Small

[11] Signal Model for PV Fed Boost Converter in Continuous and Discontinuous Conduction Modes," IEEE Transactions on Circuits and Systems II: Express Briefs, vol. 66, no. 7, pp. 1192–1196, 2019.

[12] K. Ishaque, Z. Salam, M. Amjad, and S. Mekhilef, "An improved particle

[13] swarm optimization (pso)–based mppt for pv with reduced steady-state oscillation," IEEE transactions on Power Electronics, vol. 27, no. 8,pp.3627–3638, 2012.

[14] R. W. Erickson and D. Maksimovic, Fundamentals of power electronics.

[15] Springer Science & Business Media, 2007 E. I. Batzelis, G. Anagnostou, and B. C. Pal, "A state-space representation of irradiance-driven dynamics in two-stage photovoltaicsystems," IEEE Journal of Photovoltaics, vol. 8, no. 4, pp. 1119–1124, 2018.

[16] S. Figueiredo and R. Nayana Alencar Leão e Silva Aquino, "Hybrid MPPT Technique PSO-P&O Applied to Photovoltaic Systems Under Uniform and Partial Shading Conditions," in IEEE Latin America Transactions, vol. 19, no. 10, pp. 1610-1617, Oct. 2021, doi: 10.1109/TLA.2021.9477222.

[17] E. I. Batzelis, G. Anagnostou and B. C. Pal, "A State-Space Representation of Irradiance-Driven Dynamics in Two-Stage Photovoltaic Systems," in IEEE Journal of Photovoltaics, vol. 8, no. 4, pp. 1119-1124, July 2018, doi: 10.1109/JPHOTOV.2018.2839261

[18] J M. A. Elgendy, B. Zahawi, and D. J. Atkinson, "Assessment of Perturb and Observe MPPT Algorithm Implementation Techniques for PV Pumping Applications," IEEE transactions on sustainable energy, vol. 3, no. 1, pp. 21–33, 2011.

[19] O. Ibrahim, N. Z. Yahaya, N. Saad and M. W. Umar, "Matlab/Simulink model of solar PV array with perturb and observe MPPT for maximising PV array efficiency," *2015 IEEE Conference on Energy Conversion*

(CENCON), Johor Bahru, Malaysia, 2015, pp. 254-258, doi: 10.1109/CENCON.2015.7409549.

[20] C. Ananthi and B. Kannapiran, "Improved design of sliding-mode controller based on the incremental conductance MPPT algorithm for PV applications," *2017 IEEE International Conference on Electrical, Instrumentation and Communication Engineering (ICEICE)*, Karur, India, 2017, pp. 1-6, doi: 10.1109/ICEICE.2017.8191848.

[21] A. -N. Sharkawy *et al.*, "Solar PV Power Estimation and Upscaling Forecast Using Different Artificial Neural Networks Types: Assessment, Validation, and Comparison," in *IEEE Access*, vol. 11, pp. 19279-19300, 2023, doi: 10.1109/ACCESS.2023.3249108.

[22] Subiyanto, S., Mohamed, A., and Hannan, M. (2012). Intelligent maximum power point tracking for pv system using hopfield neural network optimized fuzzy logic controller. Energy and Buildings, 51:29–38

[23] Ahmed, N. A. and Miyatake, M. (2008). A novel maximum power point tracking for photovoltaic applications under partially shaded insolation conditions. Electric Power Systems Research, 78(5):777–784

[24] Chao, K.-H., Lin, Y.-S., and Lai, U.-D. (2015). Improved particle swarm optimization for maximum power point tracking in photovoltaic module arrays. Applied Energy, 158:609–618.

[25] Manickam, C., Raman, G. R., Raman, G. P., Ganesan, S. I., and Nagamani, C. (2016). A hybrid algorithm for tracking of gmpp based on po and pso with reduced power oscillation in string inverters. IEEE Transactions on Industrial Electronics, 63(10):6097–6106.

[26] Ishaque, K., Salam, Z., Amjad, M., and Mekhilef, S. (2012a). An improved particle swarm optimization (pso)–based mppt for pv with reduced steady-state oscillation. IEEE transactions on Power Electronics, 27(8):3627–3638.

[27] Ishaque, K., Salam, Z., Shamsudin, A., and Amjad, M. (2012b). A direct control based maximum power point tracking method for photovoltaic system under partial shading conditions using particle swarm optimization algorithm. Applied Energy, 99:414–422.

[28] H. Abdel-Gawad and V. K. Sood, "Small-signal analysis of boost

converter, including parasitics, operating in CCM," *2014 6th IEEE Power India International Conference (PIICON)*, Delhi, India, 2014, pp. 1-5, doi: 10.1109/POWERI.2014.7117622.

[29] A. Shawky, H. Radwan, M. Orabi and M. Z. Youssef, "A novel platform for an accurate modeling and precise control of photovoltaic modules with maximum operating efficiency," *2015 IEEE Applied Power Electronics Conference and Exposition (APEC)*, Charlotte, NC, USA, 2015, pp. 205-212, doi: 10.1109/APEC.2015.7104353.

[30] S. J. Chiang, K. T. Chang and C. Y. Yen, "Residential photovoltaic energy storage system," in IEEE Transactions on Industrial Electronics, vol. 45, no. 3, pp. 385-394, June 1998, doi: 10.1109/41.678996.

[31] M. G. H. Omran, A. P. Engelbrecht and A. Salman, "Differential Evolution Based Particle Swarm Optimization," 2007 IEEE Swarm Intelligence Symposium, Honolulu, HI, USA, 2007, pp. 112-119, doi: 10.1109/SIS.2007.368034.

PUBLICATIONS

The work has been accepted and presented into the following publications:

1.	**Title of the Paper:**	***Investigations of Different Global Peak Tracking Algorithm for extracting Maximum power from Photovoltaic systems.***
	Author names:	[1]Ojha Mayank and [2]Vanjari Venkata Ramana
	Name of Conference:	4th International Conference Emerging Technologies (INCET - 2023)
	Name of Organizer:	Jain College of Engineering, Belagavi, Karnataka, India IEEE Bangalore Section
	Conference Date with Venue:	May 26th – May 28th, 2022 Virtual Mode
	Have you registered for the Conference?	Yes
	Status of the paper:	Accepted and Presented
	Date of Communication:	15rd April, 2023
	Date of Acceptance:	26th April, 2023
	Publication Platform:	IEEE Xplore